22

Ortuño-Arzate, S., H. Ferket, M.-C. Cacas, R. Swennen, and F. Roure, 2003, Late Cretaceous carbonate reservoirs in the Cordoba Platform and Veracruz Basin, eastern Mexico, *in* C. Bartolini, R. T. Buffler, and J. Blickwede, eds., The Circum-Gulf of Mexico and the Caribbean: Hydrocarbon habitats, basin formation, and plate tectonics: AAPG Memoir 79, p. 476–514.

Late Cretaceous Carbonate Reservoirs in the Cordoba Platform and Veracruz Basin, Eastern Mexico

Salvador Ortuño-Arzate
Instituto Mexicano del Petróleo, México, D.F., Mexico

Helga Ferket
University of Leuven, afdeling Fysico-chemische geologie, Heverlee, Belgium

Marie-Christine Cacas
Institut Français du Pétrole, Rueil-Malmaison Cedex, France

Rudy Swennen
University of Leuven, afdeling Fysico-chemische geologie, Heverlee, Belgium

François Roure
Institut Français du Pétrole, Rueil-Malmaison Cedex, France

ABSTRACT

This study focuses on the deformation history and hydrocarbon plays of Late Cretaceous carbonate reservoirs of the Cordoba Platform and adjacent Veracruz Basin. Here, the buried Laramide thrust front accounts for one of the most mature petroleum provinces of Mexico. Three regional structural cross sections across the Cordoba Platform have been constructed using available surface and subsurface geological and geophysical data, from the Sierra de Zongolica in the west to the Veracruz Basin in the east. Forward kinematic modeling of these transects, using the Thrustpack software, allowed reconstruction of the burial history of potential source rocks. One-dimensional and two-dimensional thermal modeling (using the Genex, Gentect, and Thrustpack models) allowed reconstruction of the petroleum generation history (i.e., the maturation history of potential source rocks) and the thermal evolution of carbonate reservoirs, wherein only conductive heat transfer was considered. Maximum temperatures in the Late Cretaceous reservoirs of the Cordoba Platform probably never exceeded 60°C. In contrast, the deeper duplexes located in the buried thrust front reached their maximum burial and peak temperature only very recently as a result of the Cenozoic subsidence history of the Veracruz Basin. This modeling showed that potential source rocks did not reach the oil window prior to post-Laramide episodes of burial. This means that hydrocarbons migrated essentially from east to west and upward from the Veracruz Basin and underthrusted foreland toward the productive duplexes of the buried Laramide thrust front. Microtectonic and diagenetic studies from outcrops helped in unraveling the importance of stylolite and (paleo)karst development and fracturing, and to better understand the structural control on the overall porosity and permeability of the reservoirs. Petrographic studies of outcrops and core material showed that the paleoenvironment accounts for the preservation of reasonably good matrix porosity in distinct lithofacies (i.e., in early dolomitized platform carbonates of the Orizaba and Guzmantla Formations, bioclastic wackestone to packstone in the Guzmantla Formation, and in slope breccias of the San Felipe Formation). An important factor controlling the development of secondary porosity in the Cordoba Platform carbonates appears to relate to two successive karstification episodes. The first episode was related either to global sea-level changes during the passive margin evolution or to the early development of a former Laramide flexural bulge, whereas the second karstification event postdates Laramide contractional episodes. Furthermore, hydraulic fracturing, which predates the development of bedding-parallel stylolites, is locally evidenced. They are interpreted to relate to vertical dewatering processes occurring in a dominantly extensional system. A second hydraulic fracturing postdates the bedding-parallel stylolites but predates the Layer Parallel Shortening (LPS) features. Overpressures during this second episode of hydraulic fracturing, which also locally affects the sealing strata, was mostly synchronous with the onset of the Laramide orogeny and occurred when the principal stress axis (σ_1) was already horizontal. Deformation features accounting for secondary porosity developed during the Laramide orogeny. These still act locally as vertical conduits for the fluids and eventually display fair-to-good porosity and permeability, especially in the extrados and near the lateral anticlinal closures or at places where their overall orientation is consistent with the post-Laramide (modern) stress pattern.

INTRODUCTION

Hydrocarbon exploration in foreland fold and thrust belts (FFTBs) is high risk. The tectonic complexity of these areas, the difficulty of acquiring good seismic imagery, the variation in reservoir diagenesis, and the difficulty in assessing the hydrocarbon maturation history make prediction difficult. With this awareness, the SUBTRAP Consortium project was initiated by the Institut Français du Pétrole (IFP) in 1996 with the aim of studying worldwide FFTB systems, siliciclastic as well as carbonate, to provide important guidelines for developing and validating an integrated approach to study and predict exploration risks in these frontier areas (Roure et al., 2000). The study of the Cordoba Platform and adjacent Veracruz Basin was part of this SUBTRAP project.

The Cordoba Platform is located in the eastern part of Mexico, in the western part of Veracruz State (Figure 1; Campa and Coney, 1983; Carfantan, 1986; Sedlock et al., 1993). It is made up of poorly deformed Cretaceous carbonates between the highly deformed units of the Sierra de Zongolica in the west and the Tertiary Veracruz Basin in the east. The eastern border of the Cordoba Platform constitutes a sedimentary ramp, which accounts for a transitional change toward the more basinal facies of the Veracruz Basin. From a structural perspective, this former platform margin currently relates to a major structural domain known as the buried Laramide thrust front. It involves a complex architecture of thrust faults and stacked duplexes that were tectonically accreted in the Laramide allochthon during Maastrichtian to Eocene compressional episodes. They presently are buried beneath unconformable Cenozoic siliciclastic sediments of the Veracruz Basin (Figure 2; Mossman and Viniegra, 1976; Cruz-Helu et al., 1977). Both oil and gas are produced from the Late Cretaceous carbonate reservoirs that are involved in this Laramide thrust front. Synorogenic Upper Cretaceous to Paleocene flysch deposits comprise an efficient regional seal.

Petroleum exploration was initiated in the 1920s in the Cordoba Platform and in the adjacent Veracruz

STRUCTURAL MAP OF EASTERN MEXICO

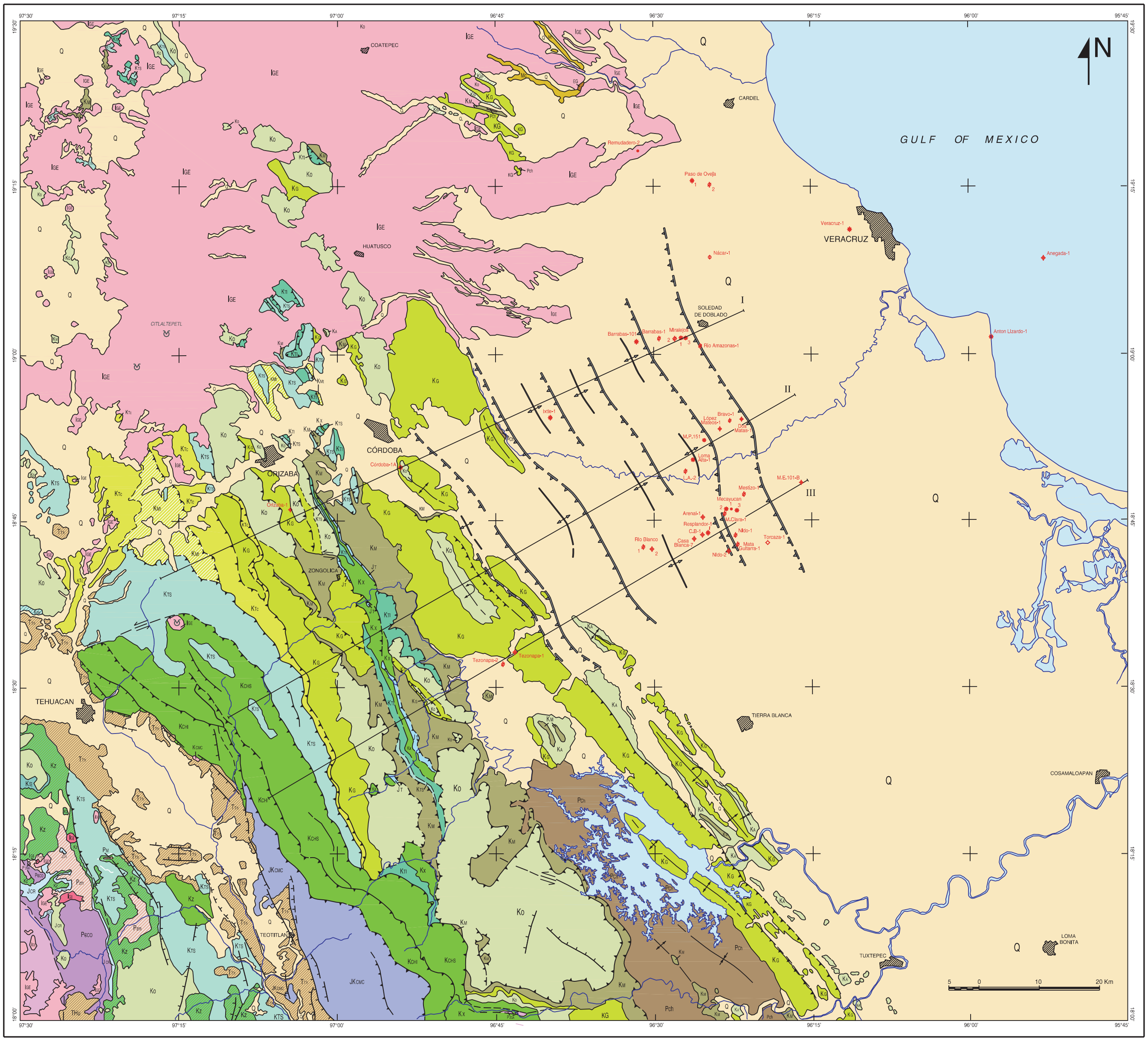

Figure 1. Synthetic geological map of the Cordoba Platform and adjacent Veracruz Basin outlining the geometry of the Laramide thrust front, as well as the locations of the SUBTRAP transects (identified as I, II, and III) and wells referred to in the text.

Basin with the well Cocuite-1. Nonetheless, most seismic surveys and drilling result from PEMEX initiatives to develop this petroleum province from 1948 onward. Since then, numerous hydrocarbon discoveries have been made in Cretaceous carbonate reservoirs along the thrust front (i.e., in the Mata Pionche, Copite, Mecayucan, Miralejos, and San Pablo fields) and in Cenozoic sandstone reservoirs in the adjacent Veracruz Basin (Table 1; Escalera-Alcocer et al., 1997; Gonzales Alvarado, 1976; Rodriguez et al., 1997).

The aim of this paper is to report on the geological-structural setting of the Cordoba Platform and Veracruz Basin and on the oil and gas prospectivity of this area. Surface geological maps, seismic profiles, and well data have been used to construct three regional structural sections across the Cordoba Platform and the adjacent foreland (Figure 2). In addition, fieldwork across two large structures, i.e., the Atoyac and Tlacuilotecatl anticlines, allowed documentation of paleostress evolution of the foothills. The nature and

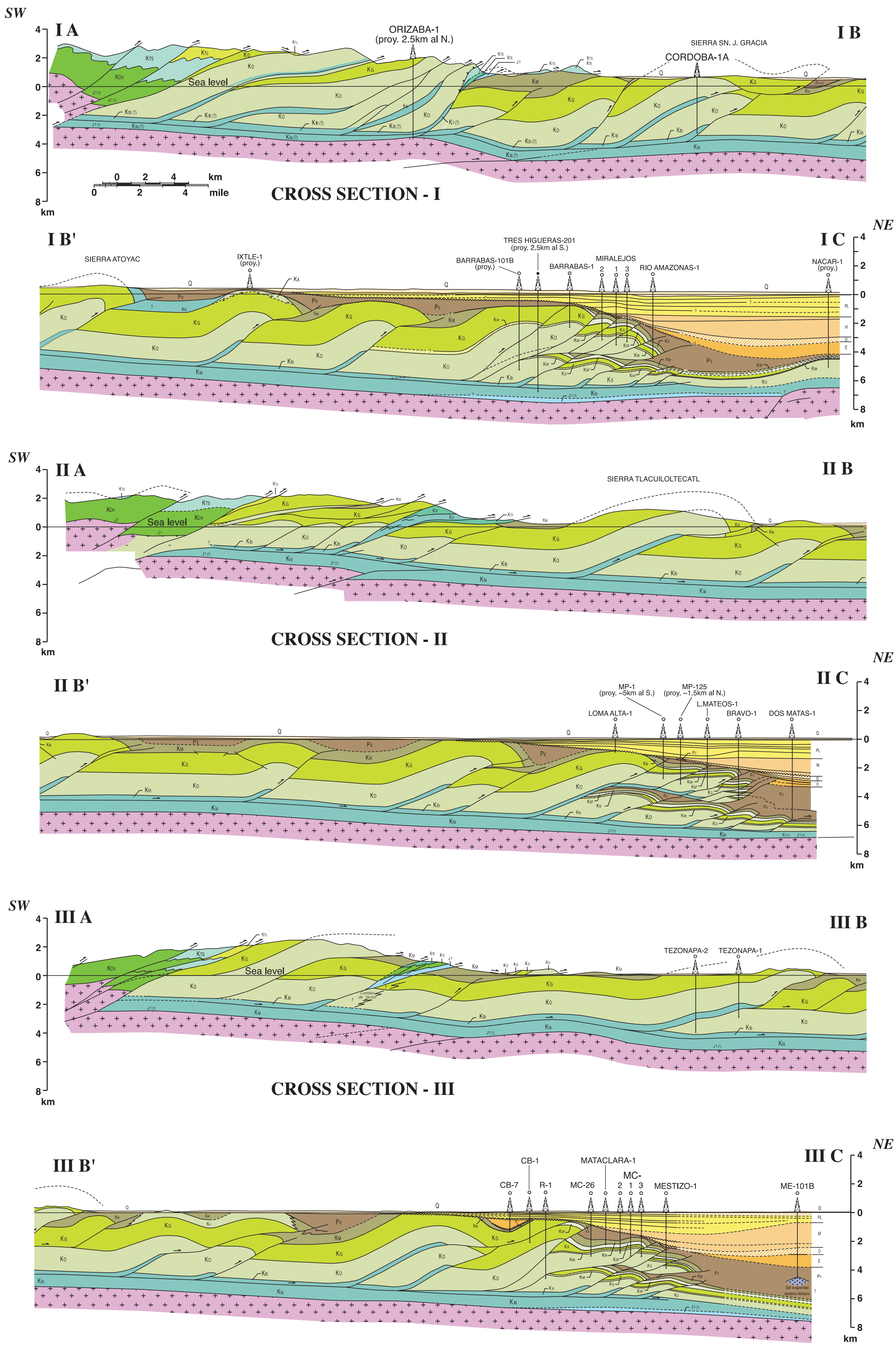
SW
I A
ORIZABA-1
(proy. 2.5km al N.)
SIERRA SN. J. GRACIA
CORDOBA-1A
I B
Sea level
km
mile
CROSS SECTION - I
I B'
SIERRA ATOYAC
IXTLE-1
(proy.)
TRES HIGUERAS-201
(proy. 2.5km al S.)
BARRABAS-101B
(proy.)
BARRABAS-1
MIRALEJOS
2 1 3
RIO AMAZONAS-1
NACAR-1
(proy.)
I C
NE
km
SW
II A
SIERRA TLACUILOLTECATL
II B
Sea level
km
CROSS SECTION - II
II B'
MP-1
(proy. ~5km al S.)
MP-125
(proy. ~1.5km al N.)
L.MATEOS-1
LOMA ALTA-1
BRAVO-1
DOS MATAS-1
II C
NE
km
SW
III A
TEZONAPA-2
TEZONAPA-1
III B
Sea level
km
CROSS SECTION - III
III B'
CB-1
CB-7
R-1
MC-26
MATACLARA-1
MC-
2 1 3
MESTIZO-1
ME-101B
III C
NE
km

Table 1. Hydrocarbon discoveries in the Cordoba Platform and adjacent Veracruz Basin.

MAIN PETROLEUM FIELDS	*PRODUCTION MMBOE*	*DISCOVERY DATE*
Mata Pionche	121.0	1974
Mecayucan	109.3	1976
Cópite*	89.8	1974
Angostura*	32.5	1953
Rincón Pacheco*	17.2	1957
Miralejos*	16.8	1977
San Pablo*	12.5	1956
Nopaltepec*	6.0	1957
M. R. Aguilar*	1.6	1976
Tres Higueras*	0.7	1955
Plan de Oro*	0.3	1973
Colón*	0.01	1966
Casa Blanca*	0.09	1954
Remudadero*	0.07	1978
Cocuite**	7.604	1962
Veinte**	0.8	1968
Novillero**	2.9	1966

**Mesozoic reservoir; **Cenozoic reservoir.*
Source: Pemex-IMP, Internal Reports, 1995.

distribution of mesoscopic features (e.g., stylolitic planes, tensional joints, faults,) in the Late Cretaceous reservoir intervals were recorded. This also was an opportunity to sample oriented plugs with cemented microstructures in order to trace the evolution of paleofluids and diagenetic cements with respect to the deformational evolution and orientation of individual sets of microstructures. In addition, data on source-rock potential and the effect on the evolution of diagenesis in the dual porosity system will be addressed.

GEOLOGICAL SETTING

Based on reconstruction of three regional transects through the Orizaba and Cordoba Platforms and the Zongolica and Veracruz Basins (Figure 1), and relying on seismic data and a large number of wells, it was possible to differentiate the major tectonic units and to infer the structural style of the Cordoba Platform and Veracruz Basin (Ortuño, 1989, 1991; PEMEX-IMP, 1995). This allowed definition of the major tectonic units and elucidation of the pre-, syn- and postorogenic history of major reservoir and source-rock intervals.

Major Tectonic Units and Structural Style of the Cordoba Platform and Veracruz Basin

The Cordoba Platform constitutes a major tectonic unit, which is directly overthrust by tectonic outliers of the Orizaba Platform in the southwestern part of the studied area (Figures 1 and 2). In the north, however, narrow north- to northwest-trending tectonic slices made up of Late Jurassic to Late Cretaceous basinal series of the Zongolica succession have been preserved and are intercalated between these two platformal assemblages. In the northern part of the studied area (Figure 1), the Laramide thrust front is located in the Cordoba Platform, which is partly attached to the autochthonous foreland farther to the northeast. Elsewhere, the Laramide thrust front is superimposed on the former platform-to-basin transition, and the Cordoba Platform is currently thrust eastward over the basinal facies of the Veracruz Basin.

Upper Cretaceous carbonates of the Orizaba Platform have been detached entirely from their substratum and constitute a large tectonic outlier, named "the Orizaba–Cerro Rabón" allochthon, in the southwestern part of the studied area. The Upper Jurassic and Lower Cretaceous series of the former Zongolica Basin are well exposed in the tectonic slices along the western part of the cross sections, overlying an intra-Jurassic décollement level. In contrast, the basal décollement level of the Cordoba Platform probably relates to a Lower Cretaceous evaporitic series. In addition, Late Cretaceous and Paleocene flysch series constitute a shallower decoupling horizon. Thus, the overall structural style of the Cordoba Platform, consisting of large ramp anticlines, is controlled by the thickness of the intervening brittle layer that is made up of middle to Late Cretaceous platform carbonates. Western limbs of these anticlines usually dip gently toward the west, whereas the eastern limbs are commonly subvertical (Figure 2). Because of lateral facies and thickness changes at the former platform-to-basin transition, the frontal part of the Laramide allochthon displays a distinct structural style, with narrower spacing between thrusts, resulting in an antiformal

Figure 2. Structural cross sections across the Cordoba Platform (see location of these three SUBTRAP sections in Figure 1). Notice that each transect has been split into two parts (A-B and B′-C). J = Jurassic; K = Cretaceous; K_I = Lower Cretaceous; K_O = Orizaba Formation; K_{Mt} = Maltrata Formation; K_G = Guzmantla Formation; K_{SF} = San Felipe Formation; K_M = Mendez Formation; P_V = Paleocene Velasco Formation; E = Eocene; O = Oligocene: M = Miocene; PL = Pliocene; Q = Quaternary.

stack of duplexes. However, unlike classical triangle zones, the upper tectonic unit is directly overlain by a major unconformity that postdates the Laramide episodes of tectonic contraction. There is no evidence of any regional backthrust developed at the front of the tectonic wedge (Figure 2).

Although entirely located in the autochthonous foreland of the Laramide orogen, the Veracruz Basin contains recent near-surface anticlines, which deform even the Neogene sequence, attesting to the occurrence of post-Laramide tectonic episodes (Figure 3). However, as evidenced on seismic imagery, these structures do not connect with the foothills; they are strictly localized near major, basement-involved, high-angle faults. These deep basement structures probably relate to the Jurassic opening of the Gulf of Mexico, but they also have been reactivated as normal, reverse, or strike-slip faults during post-Laramide evolution of the margin.

Pre-, Syn-, and Postorogenic History

Pre-Cretaceous History

Although the main regional rifting event of the Gulf of Mexico and adjacent areas is reported to be Jurassic in age (Freeland and Dietz, 1971; Walper and Rowett, 1972; Moore and del Castillo, 1974; Aubouin et al., 1977, 1980; Córdoba et al., 1980; Pindell and Dewey, 1982; Anderson and Schmidt, 1983; Burke et al., 1984; Buffler and Sawyer, 1985; Salvador, 1987, 1991; Winkler and Buffler, 1988; Burkart and Scotese, 1992), pre-Cretaceous sedimentary strata are recorded in the studied area only in former basinal paleogeographic domains, such as the Zongolica and Veracruz Basins, which developed west and east of the Cordoba Platform, respectively (Figures 4, 5, and 6). Although the Mesozoic sequence of the Veracruz Basin still is part of the autochthonous foreland, it is buried beneath thick Cenozoic sediments that hamper any direct observation of its lithostratigraphic assemblage. In contrast, coeval Jurassic to Upper Cretaceous series of the former Zongolica Basin currently are exposed in the Sierra de Zongolica. In the intervening Cordoba and Orizaba Platform domains, Cretaceous platform carbonates of the former passive margin rest directly on a late Carboniferous to Permian crystalline basement (with radiometric ages of 323 m.y. measured by K-Ar methods on granitic plutons; Jacobo, 1995). Depth to the basement increases progressively from 3000 m in the west up to 6000 m in the east, according to numerous wells (i.e., Remudadero, Paso de Ovejas, Orizaba, and Actopan). The same type of basement also is assumed to extend beneath the Veracruz Basin.

Beneath the former Orizaba and Cordoba platformal domains, only localized and poorly dated red beds, including both sandstones and conglomerates, have been documented in some wells (i.e., Paso de Ovejas, Remudadero, and Actopan), and, thus, are assumed to record remnants of the synrift sequence (Figure 5).

The Passive-margin Sequence of the Cordoba Platform

Postrift sedimentation resulting from the thermal subsidence of the Gulf of Mexico margins is well recorded here by the thick Cretaceous carbonate sedimentation in the Cordoba Platform (Menes, 1980; Carrasco, 1978; Toriz, 1985, 1987; Ortuño, 1991).

The basal portion of the Lower Cretaceous platform series is Neocomian to Aptian in age. These strata are made up of light-gray limestones, including both mudstone and wackestone, which are locally dolomitized. They grade upward into dolomite and dolomitic limestones with evaporitic interbeds that display early dissolution features and relatively good matrix porosity (3 to 10%). Their depositional environment relates to an inner carbonate platform. This sequence is as much as 1000- to 1500-m thick. It is assumed to rest directly on top of the crystalline basement in most parts of the Cordoba Platform. However, it has been drilled in only a limited number of wells (i.e., in Tezonapa-1 and -2 and Cerro de Oro-1).

The middle Cretaceous Orizaba Formation is made up of an Albian to Cenomanian platform sequence, which is 1500- to 2000-m thick in the central and western part of the Cordoba Platform. It becomes thinner eastward along the buried Laramide thrust front. Because of the underlying Lower Cretaceous evaporitic layers, this portion of the Cretaceous carbonate section of the Cordoba Platform frequently is detached from its underlying substratum. Its lithology can be studied in a number of wells and outcrops, from the Sierra de Zongolica in the west to the buried Laramide thrust front in the east (e.g., Orizaba-1, Tezonapa-1 and -2, Córdoba-1A).

The lower part of the Orizaba Formation consists of light-gray limestones, comprising mudstones and packstones with numerous bioclasts, especially miliolids (Plate IA), as well as dolomitic limestones and dolomite (Plate IB). In contrast, the upper part of the formation is not dolomitized. The depositional environments still relate to an inner, dominantly carbonate

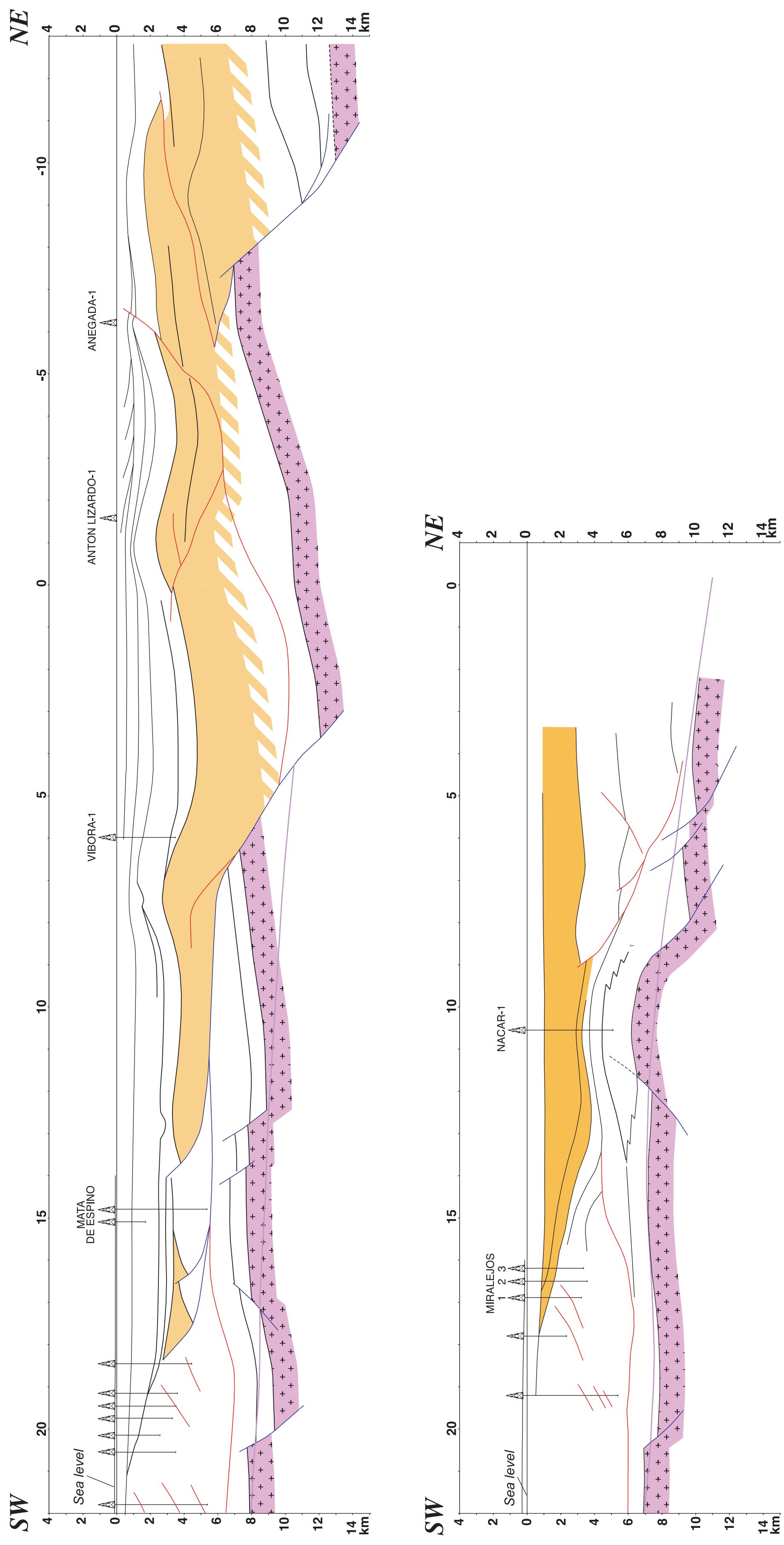

Figure 3. Structural cross sections across the tectonic front zone and the adjacent Veracruz Basin, directly on line with the SUBTRAP transects.

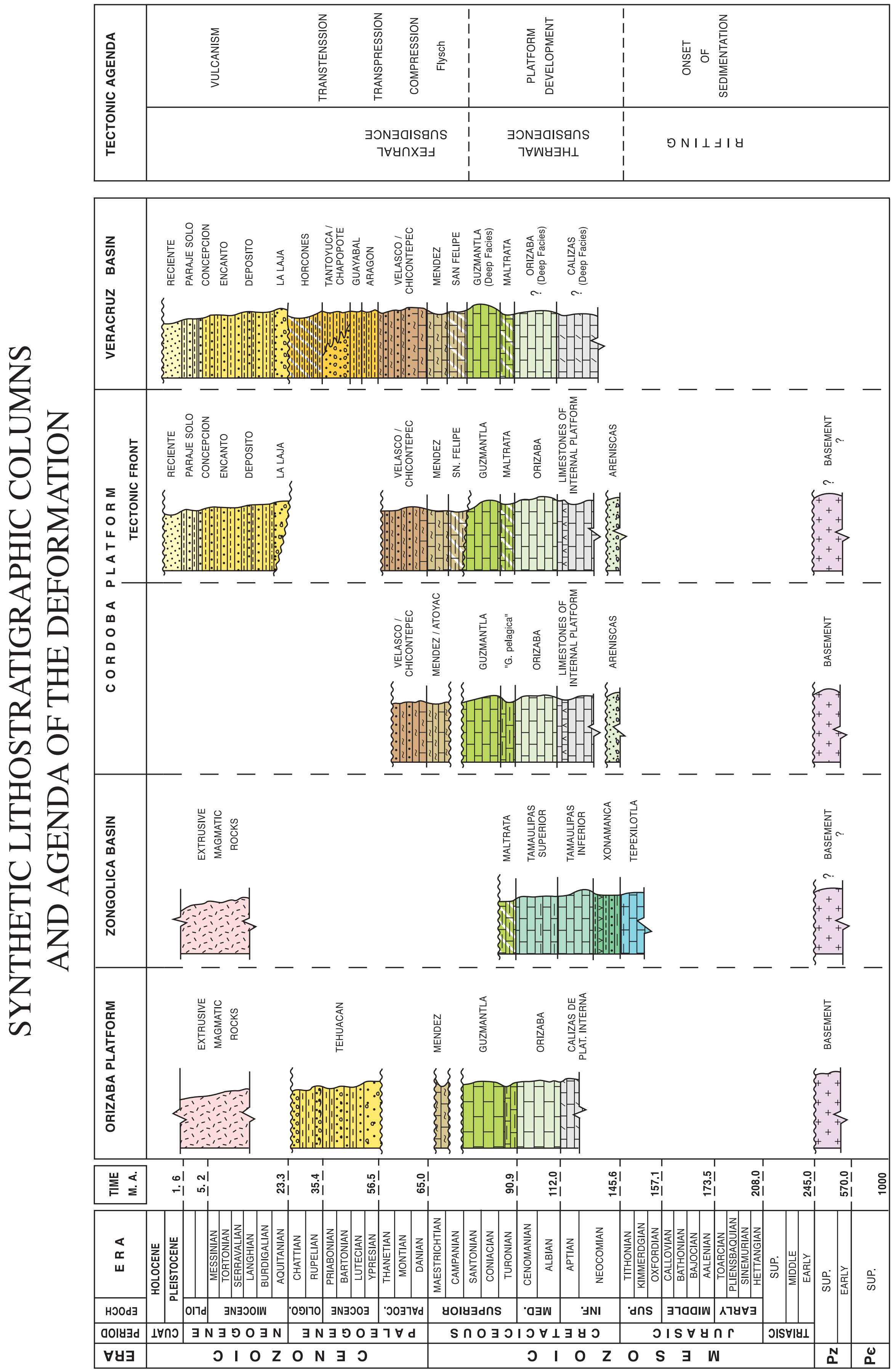

Figure 4. Synthetic lithostratigraphic columns of the Cordoba Platform and adjacent paleogeographic domains (for legend, see Figure 5).

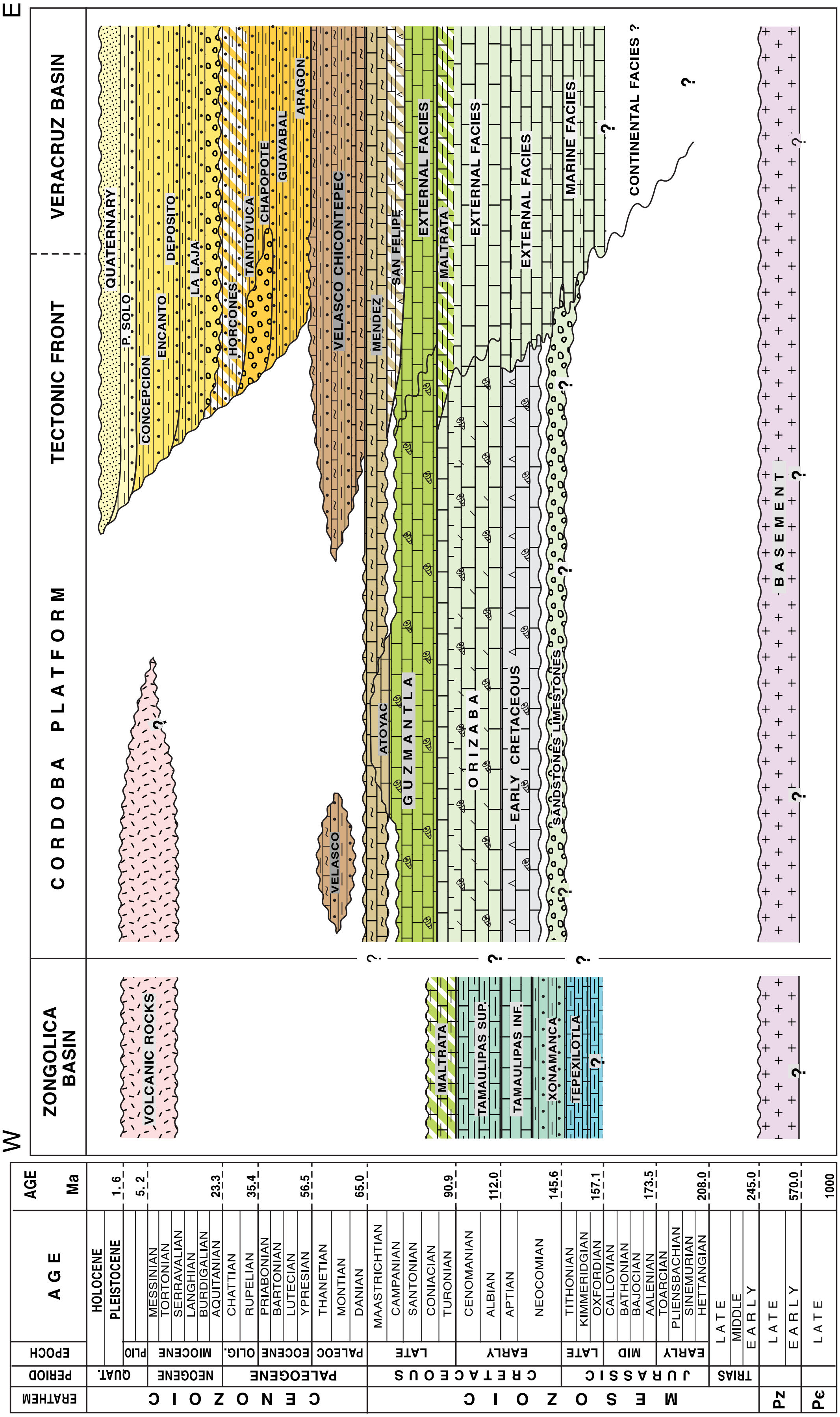

Figure 5. Synthetic lithostratigraphic columns of the Cordoba Platform and adjacent paleogeographic domains.

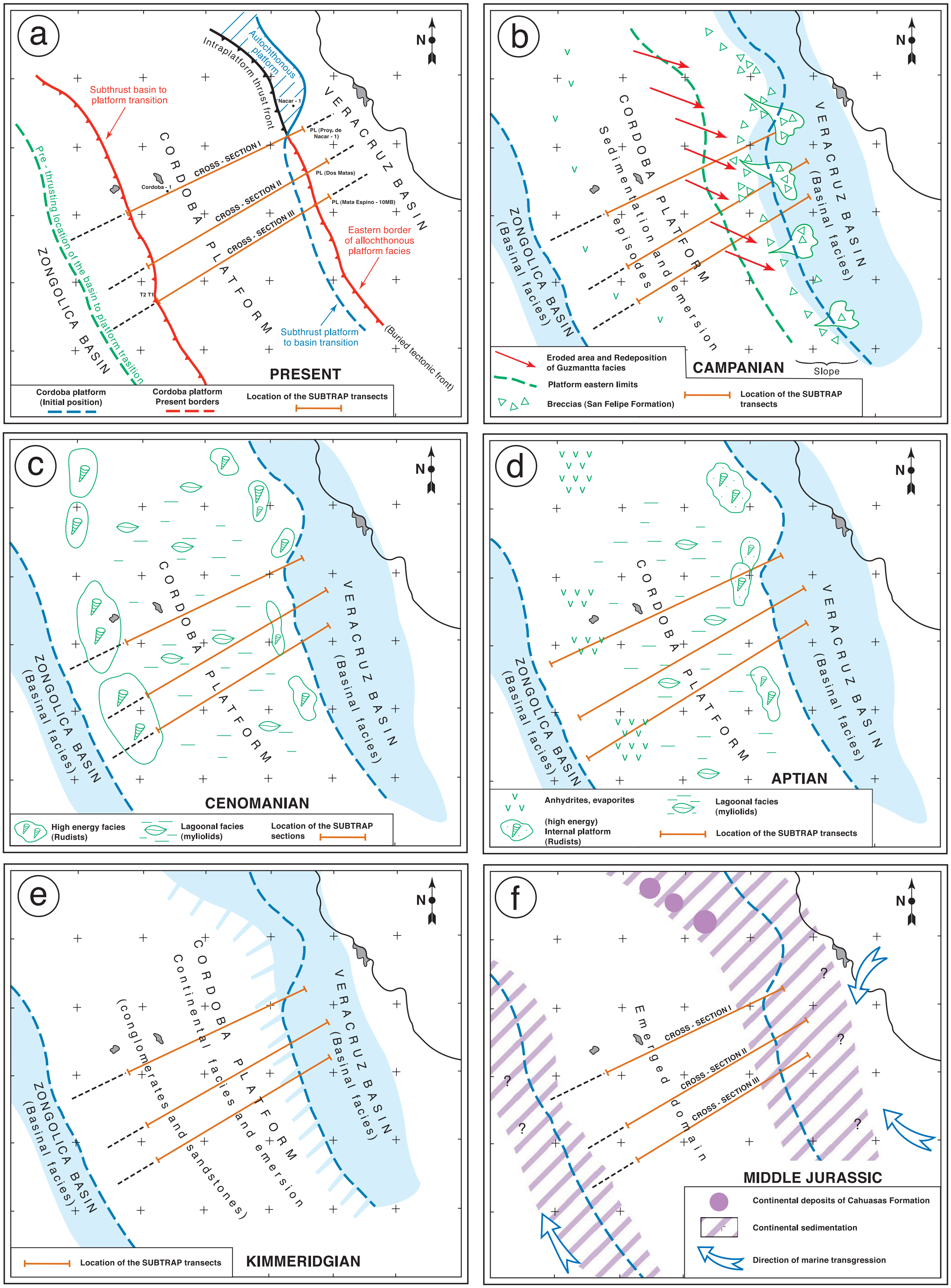

Figure 6. Paleogeographic maps of the Cordoba Platform and adjacent domains.

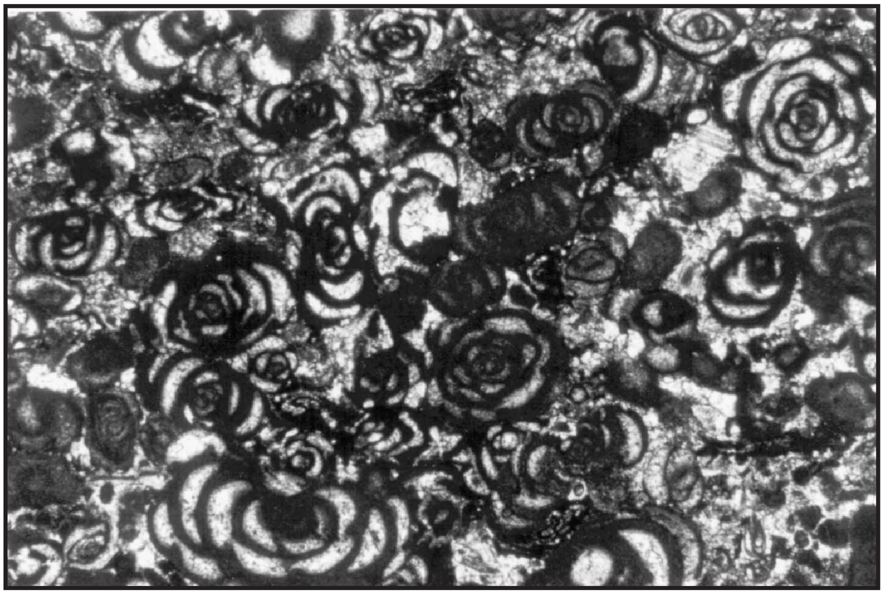

I A

Plate I. Overview of different lithologies (A to G: photomicrographs; H: core photograph; scale 1cm = 312 μm if not otherwise stated). (A) Orizaba Formation, miliolid packstone (Nido 2 borehole). (B) Orizaba Formation, medium-crystalline dolomite with high porosity (white areas; Tlacuiloltecatl Anticline).

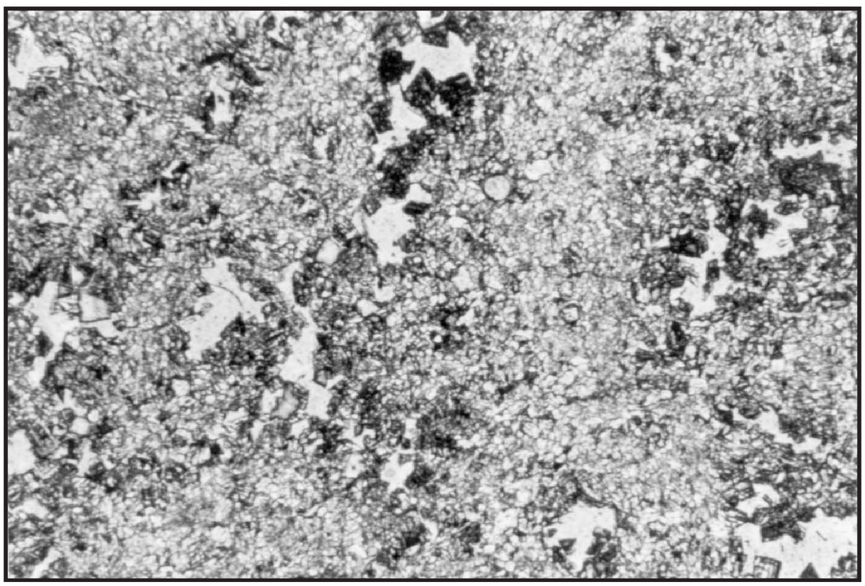

I B

platform (Figure 6). Transition to evaporitic facies occurs along the southwestern border of the Cordoba Platform, whereas elsewhere, the main lithotypes reflect isolated intraplatform lagoonal settings (Toriz, 1985; Ortuño, 1989, 1991).

Unlike the Lower and middle Cretaceous, the Upper Cretaceous carbonate sequence has been subdivided into a number of formations, some of them coeval in age but of distinct paleoenvironmental affinities. The sequence includes:

1) the Guzmantla Formation, which comprises (a) a Turonian lower unit composed of well-bedded limestones and argillitic limestones with a few dolomitized horizons and with mudstones and wackestones that record the depositional environments of an outer platform (Plate IC); and (b) a Coniacian-Santonian upper unit displaying thicker beds comprising partly dolomitized light-gray limestones with wackestones and packstones (Plate ID and IE) that represent an inner-platform paleoenvironment with isolated lagoons (Figure 6).

Although the Guzmantla Formation reaches a thickness of 1500 m across the Cordoba Platform, it becomes progressively thinner eastward toward the buried Laramide thrust front and Veracruz Basin, as a result of both a paleogeographic change toward more basinal facies and subsequent Late Cretaceous erosional episodes.

Plate I. (cont.) (C) Guzmantla Pelagic Formation, wackestone with dominantly planktonic foraminifera (Nido 2 borehole). (D) Guzmantla Formation—lower unit, wackestone with debris of rudist shells; scale 1cm = 625 μm (Tlacuiloltecatl Anticline).

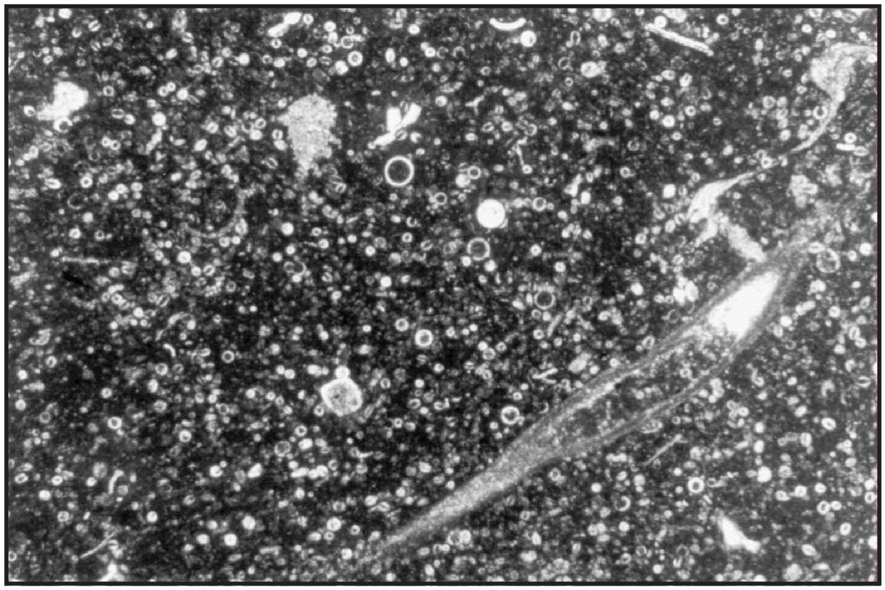

I C

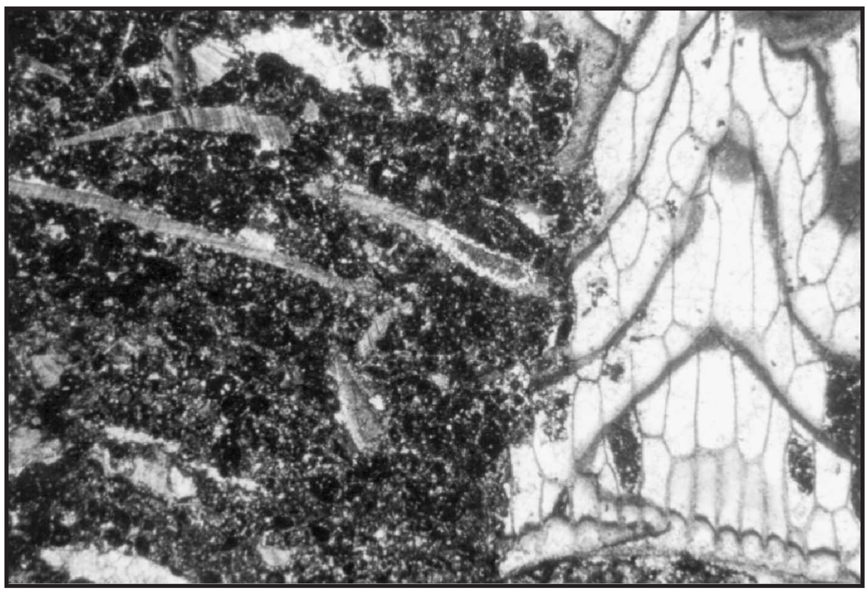

I D

2) the Maltrata Formation of Turonian age. These strata are well-bedded dark limestones and argillaceous limestones, including both mudstones and argillitic wackestones (Plate IF) with a high organic content (TOC varying between 3 and 5%). This unit is 100- to 400-m thick. It displays transitional facies toward the deeper-water depositional environments of the Veracruz Basin, but as such, it is restricted to the eastern margin of the Cordoba Platform, as seen in numerous wells (e.g., Miralejos-1, −2, and −3; Mecayucan-1 and −2; and Matapionche-1) near the buried Laramide thrust front.
3) the Atoyac Formation of Campanian-Maastrichtian age. These strata are made up of light-colored, medium- to coarse-grained limestone beds, including packstones and grainstones with numerous bioclasts (Plate IG), recording high-energy depositional environments. The formation constitutes the uppermost part of the carbonate platform and is overlain directly by a Late Cretaceous to Paleocene flexural flysch sequence. The Atoyac Formation reaches a thickness of 300 to 400 m; however, because of subsequent erosion, this part of the section is preserved only in the structural lows of the Cordoba Platform.
4) The San Felipe Formation, of middle to late Campanian age, is restricted to the eastern margin of the Cordoba Platform in the vicinity of the buried Laramide thrust front. This sequence consists of slope breccias (Plate IH) comprising reworked fragments of the Guzmantla Formation,

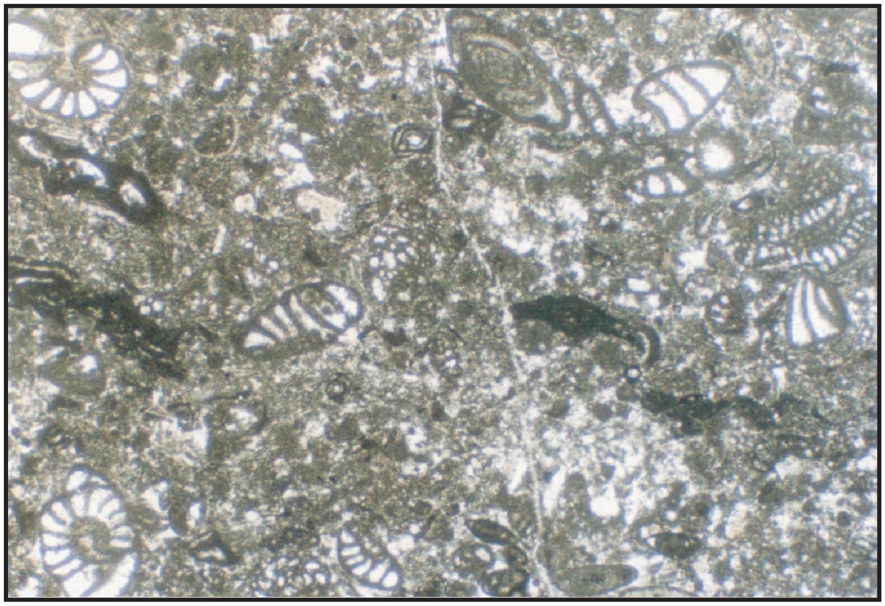

I E

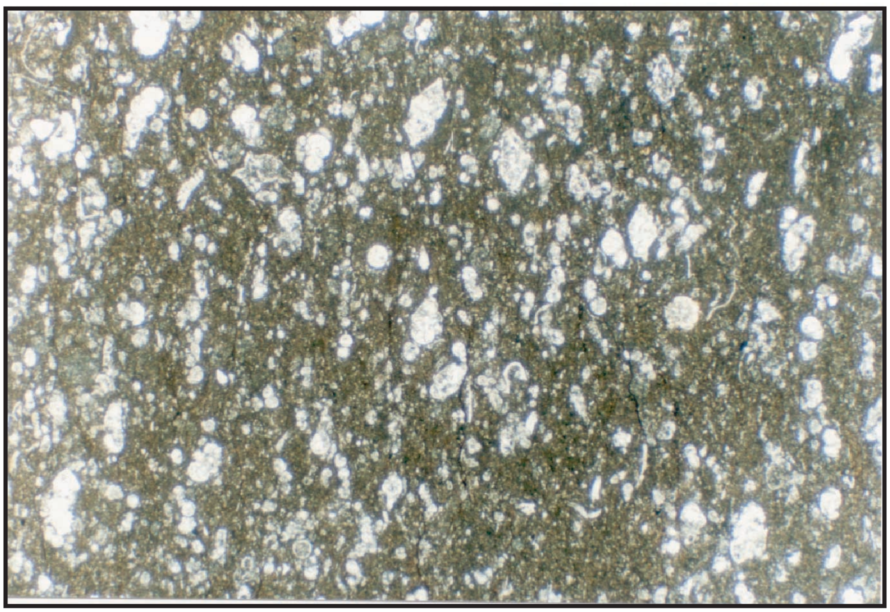

I F

Plate I. (cont.) (E) Guzmantla Formation— upper unit, wackestone to packstone with miliolids, orbitulina, and fusulinids (Atoyac anticline). (F) Maltrata Formation, laminated wackestone with globotruncana (Nido 2 borehole).

which is derived from the erosion of the Cordoba Platform, and flysch deposits. The sequence was deposited synchronously with the first episodes of deformation. The Cordoba Platform was at that time locally emergent at the former location of the flexural bulge, where major paleokarst developed. Erosional channels that cut across older carbonate facies are filled with carbonate breccias, which grade upward into preflysch and flysch deposits, with interbedded limestones, argillitic limestones, and marly argillites. The basal part of this sequence displays good porosities (3 to 7%) and corresponds to the main productive horizon in the subsurface.

Syn-orogenic Series and Deformation History of the Cordoba Platform

The Cordoba Platform is located at the southern end of the Sierra Madre foothills, which developed during the Cordilleran-Laramide orogeny (Armstrong, 1974; Coney, 1978; Carfantan, 1986; De Cserna, 1989; Ortega-Gutierrez et al., 1990; Feng et al., 1995; Pottorf et al., 1996).

Onset of tectonic contraction and foreland flexure occurred during the late Campanian along the western margin of the Cordoba Platform. However, the coeval San Felipe Formation, which was deposited during the same time interval farther east, adjacent to the Veracruz Basin, still was carbonate dominated.

Plate I. (cont.) (G) Atoyac Formation, bioclastic packstone to grainstone with foraminifera and rudist fragments. In the right portion, a karst dissolution vug is cemented by equant calcite; scale 1cm = 625 μm (Atoyac anticline). (H) San Felipe Formation, slope breccia (Tejeda 1 borehole).

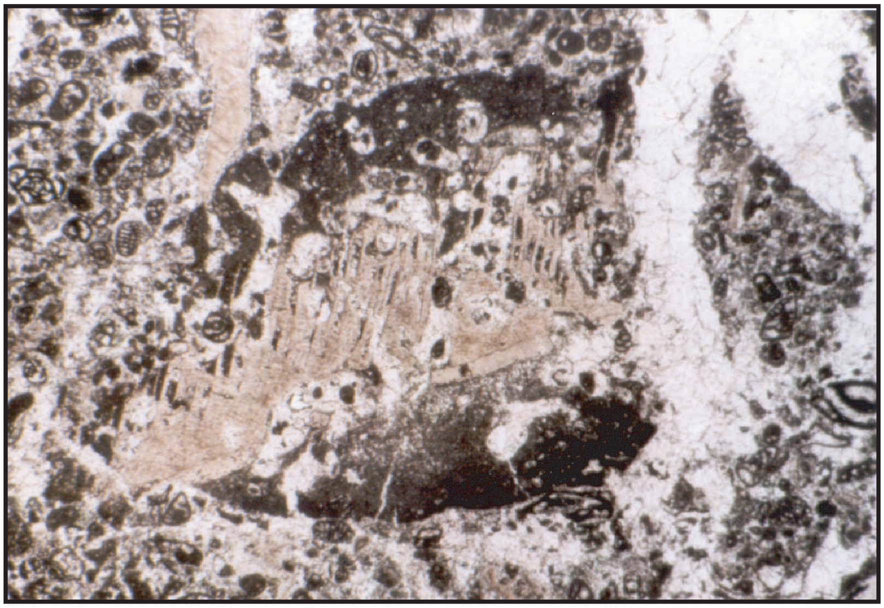

I G

I H

Other Late Cretaceous to Paleocene syn-orogenic deposits also are well developed in the structural lows, i.e., in areas where they have been preserved during subsequent erosional episodes. They comprise:

1) the Mendez Formation of Maastrichtian age. It is made up of turbiditic flysch deposits of carbonate and siliciclastic composition containing reworked fragments of the platform and siliciclastic debris of the orogen. It is assumed that this formation initially was deposited over the entire Cordoba Platform and adjacent domains. Because of subsequent erosion, this formation is no longer preserved in the anticlinal outcrops of the Zongolica thrust belt. Its residual thickness is, therefore, highly variable. It can locally reach as much as 300 m, and it constitutes a good seal for underlying Cretaceous reservoirs in the buried Laramide thrust front.
2) the Velasco-Chicontepec Formation of Paleocene age. This series is more quartzose than the Maastrichtian flysch. It is made up dominantly of fine-grained sandstone and argillite, with a minor carbonate fraction. It also comprises deep-water flysch deposits, currently preserved only in the structural lows of the Cordoba Platform. This formation is well preserved in the buried Laramide thrust front and across the Veracruz Basin.

Postorogenic Series and Evolution of the Veracruz Basin

Because of regional uplift and erosion, no syn- or postorogenic sediments currently are preserved above the allochthon except in the vicinity of the buried Laramide front, where Neogene sediments progressively onlap the former erosional surfaces (Figure 2). In addition, regional tilting toward the east currently is observed in the basement beneath the Cordoba Platform. This tilting is not consistent with the former development of a Laramide foreland flexure, but rather it is similar to the overall geometry of the Pliocene unconformity that has the same gentle, east-dipping attitude. Therefore, it is assumed that most of the uplift and erosion of the Cordoba allochthon postdate the Laramide orogeny and, thus, do not relate to the tectonic contraction. This differential vertical motion, with uplift in the west and active subsidence in the east, is probably related to more global lithospheric processes operating during the post-Laramide and involving a progressive rise of the asthenosphere beneath this portion of the Mexican margin of the Gulf of Mexico. Since the end of the Laramide orogeny, the studied area indeed constitutes a back-arc domain with respect to the still-active Pacific margin and Pliocene-Quaternary trans-Mexican volcanic arc (Molnar and Sykes, 1969; Anderson and Silver, 1974; Campa et al., 1974; Aubouin et al., 1977, Córdoba et al., 1980; Wadge and Burke, 1983; Carfantan, 1986; De Cserna, 1989; Ortega-Gutierrez et al., 1990; Suter, 1991; Reed, 1994).

In contrast to the Cordoba Platform, a Paleogene and Neogene sequence as much as 10-km thick was deposited and has been preserved in the adjacent Veracruz Basin. This section records post-Laramide regional kinematics.

1) Although the Jurassic to Paleocene series of the Veracruz Basin have never been drilled, they are likely to be of a basinal type, as indicated by the platform-to-basin facies transitions observed in the wells of the buried Laramide front along the eastern margin of the Cordoba Platform. As such, they are likely to comprise good potential source rocks in the Kimmeridgian and Turonian sequences.
2) Based on seismic data, short inversion and transpressional episodes occurred during the Eocene-Oligocene and Neogene. Localized near major basement-involved, high-angle faults, they account for local anticlinal closures in the Veracruz Basin (Figure 3). It is unlikely, however, that they control any major deformation or fault reactivation in the Cordoba allochthon, which shows no post-Laramide subsidence or Cenozoic sedimentation.
3) Eocene to Neogene episodes of alternating active thermal subsidence and regional extension are seen on seismic imaging as the reactivation of basement-involving high-angle faults that control the location of major depocenters. As mentioned above, this renewed Cenozoic rifting of the Veracruz Basin is largely superimposed on the former Jurassic rift system of the Gulf of Mexico and probably resulted from global dynamics in the hanging wall of the Pacific subduction.

Eocene to Neogene series were penetrated in several wells and display the following features:

1) The Eocene series is made up of medium- to fine-grained sandstones and argillites, mostly devoid of carbonates. Its thickness is between 500 and 1500 m in the vicinity of the buried Laramide front, but, according to seismic data, it could be significantly thicker in the main depocenters of the Veracruz Basin. The Eocene sequence itself has been subdivided into the Aragon, Guayabal, Chapopote, and Tantoyuca Formations.
2) The Oligocene series (i.e., the Horcones Formation) also consists of sandstones and argillites. This sequence thins westward and locally rests unconformably on Eocene and Paleocene strata in the vicinity of the buried Laramide front (Figure 2).
3) The Miocene series also comprises sandstone and argillaceous assemblages that are subdivided into a number of formations, including the La Laja Formation, with a basal conglomerate and medium-grained sandstones; the Deposito and Encanto Formations, made up of sandstones; and the Concepción Formation, consisting of sandstone and argillite. These Miocene units locally rest unconformably on deformed Paleocene flysch sequences in the vicinity of the buried Laramide front (Figures 2 and 3). Changes observed in the average granulometry likely relate to increasing subsidence rates during the Miocene.
4) Pliocene strata record the last episodes of marine sedimentation but also display fluvial and brackish deposits (Internal, unpublished reports, PEMEX and IMP; López, 1979). This is the Paraje Solo Formation, comprising sandstone and argillite. In contrast, the most recent deposits consist of sandy argillite.

KINEMATIC MODELING

Construction of Regional Structural Sections

The seismic lines used to constrain the structural sections were good enough to trace the basal décollement level beneath the widest synclines of the Cordoba allochthon. This also gives some confidence for the two-way time depth to the crystalline basement. Notice that depth conversions were addressed manually, with the basic assumption that any change in the basement attitude beneath the anticlines was likely a result of velocity pull-up rather than high-angle faults.

In these reconstructions, the possible occurrence of localized Jurassic grabens beneath the basal intra-Cretaceous décollement of the Cordoba Platform was not taken into account. Ultimately, if any of these early depocenters existed, they probably would contain continental red beds rather than Kimmeridgian source rocks, thus precluding any direct incidence on the regional petroleum systems. Alternatively, such red beds have been found locally by drilling in the autochthonous foreland (i.e., in the Nacar well). However, these siliciclastic horizons could have been an exotic source of fluids during the hydrothermal diagenesis of the overlying Cretaceous carbonates.

In contrast to the poor-quality seismic lines that cross the Cordoba Platform, the seismic data improves significantly over the buried Laramide front and adjacent parts of the Veracruz Basin. Nevertheless, due to the great thickness of Cenozoic deposits and the lack of deep seismic imagery, direct control on the depth and architecture of the crystalline basement in most parts of the Veracruz Basin is still missing. Ultimately, gravimetric data and the overall architecture of Cenozoic depocenters and inversion features have been used here to propose a reasonable scenario for basement-cover relationships in the eastern part of the transects (Figure 3; Mossman and Viniegra, 1976; Ortega-Gutierrez et al., 1990).

2-D Forward Kinematic Evolution and Reconstruction of Burial Curves of the Carbonate Reservoirs

Once depth converted, the three regional transects were balanced and restored to their preorogenic configuration in order to provide key constraints for subsequent ''Thrustpack'' forward kinematic simulations. The restored sections are indeed necessary to provide the initial length or spacing of future thrust faults and the thickness of the passive margin, whereas the structural sections are used as target templates to control the thickness of syn-orogenic deposits and erosional profiles, as well as the final architecture of the thrust system. Incremental deformation was applied to the sections in association with foreland sedimentation, hinterland erosion, and regional flexure using a discrete number of intermediate stages to simulate the successive geodynamic and tectonic episodes recorded in the Cordoba allochthon since the onset of the Laramide orogeny (Table 2). After a trial-and-error process, the resulting sections obtained with Thrustpack ultimately compared adequately with the target templates (i.e., with the present geometries derived from the geological and geophysical data). This means that they are providing consistent kinematic pathways between the preorogenic and present configuration of the transects. Thus, they can be used directly to compute burial curves of selected reference points; i.e., the Late Cretaceous reservoir sequences of the autochthon, frontal duplexes, and surface anticlines of the Cordoba Platform (Figures 7, 8, and 9).

THE PETROLEUM SYSTEM

Source-rock Potential

Potential source-rock horizons have been documented from the Cordoba Platform and adjacent Veracruz Basin in the following sequences (Gonzales and Holguin, 1992; Guzman-Vega and Mello, 1994; Holguin-Quiñones and Roman-Ramos, 1997; and internal, unpublished reports of PEMEX and IMP.): (1) Upper Jurassic argillaceous limestones of the Tepexilotla Formation and coeval series, which are dominantly Kimmeridgian in age with basinal affinities. Although found in the western part of the Cordoba Platform allochthon, they relate to a distinct pre-Cretaceous basinal paleogeographic domain, the so-called Zongolica Basin, which once extended between the two former basement highs developing at the future location of the Orizaba and Cordoba Cretaceous platforms (Figures 2 and 6). A few wells also have penetrated Kimmeridgian source rocks in the northern part of the Veracruz Basin (i.e., near the eastern border of the Cordoba Platform). Thus, although not yet drilled there, Upper Jurassic source rocks are assumed to extend in the subsurface beneath the buried Laramide thrust front and eastward across the entire Veracruz Basin. According to Rock-Eval studies, this Upper Jurassic source rock displays high TOC and Type-II marine kerogen (Table 3); (2) Lower Cretaceous argillaceous limestones and coeval organic-rich horizons associated with evaporites, which are

Table 2. Major tectonic and geodynamic stages used for the ''Thrustpack'' forward kinematic modeling.

Stage 1 (65 to 60 m.y).	Paleocene	Onset of the Laramide deformation in the hinterland.
Stage 2 (60 to 56.5 m.y.)	Paleocene	Deformation propagates across the Cordoba Platform.
Stage 3 (56.5 to 50 M.y)	Eocene	Frontal deformation reaches its present location.
Stage 4 (50 to 42 M.y).	Eocene	Emergence and erosion of the Cordoba Platform; Continuous sedimentation in the Veracruz Basin.
Stage 5 (42 to 35 M.y).	Eocene	Emergence and erosion of the Cordoba Platform.
Stage 6 (35 to 23 m.y.)	Oligocene	Sedimentation resumes in the Veracruz Basin.
Stage 7 (23 to 5 m.y.)	Miocene	Erosion and karstification in the Cordoba Platform; Minor inversion and transpression in the Veracruz Basin.
Stage 8 (5 to 0 m.y.)	Pliocene-Quaternary	Erosion and karstification in the Cordoba Platform; Sedimentation resumes in the Veracruz Basin.

dominantly Neocomian-Aptian in age. This potential source rock has been seen in a few wells, both in the western and eastern Cordoba Platform; and (3) middle Cretaceous argillaceous limestones of the Orizaba and Maltrata Formations, which represent deep-water facies in the eastern part of the Cordoba Platform and in the adjacent Veracruz Basin.

In addition to these potential source-rock horizons, which occur along both the western and eastern platform margins, coeval deeper-water facies of the Veracruz Basin also are likely to have contributed to the known petroleum accumulations.

Thermal Modeling of the Cordoba-Veracruz Transects

Present Thermal Regime of the Cordoba Platform and Veracruz Basin

Modern geothermal gradients still are relatively low (Figure 7) in both the Cordoba Platform and the Veracruz Basin, although these areas are near the trans-Mexican volcanic axis. Bottom-hole temperatures (BHT) used for calibration of the thermal models are given in Figure 7. The relatively low geothermal gradient probably is caused by a number of independent factors, such as: (1) The crustal thickness beneath the Cordoba Platform probably was little modified during the Jurassic rifting event compared to nearby basinal domains, such as the Zongolica and Veracruz Basins. Moreover, the development of a paleokarst and modern karst is likely to contribute to active circulation of meteoric water, which, in turn, is likely to cool the underlying series. (2) Although the Veracruz Basin recorded renewed episodes of rifting during the Tertiary, it was also the site of rapid sedimentation. Consequently, the thick Cenozoic sedimentary pile is likely to account for a regional

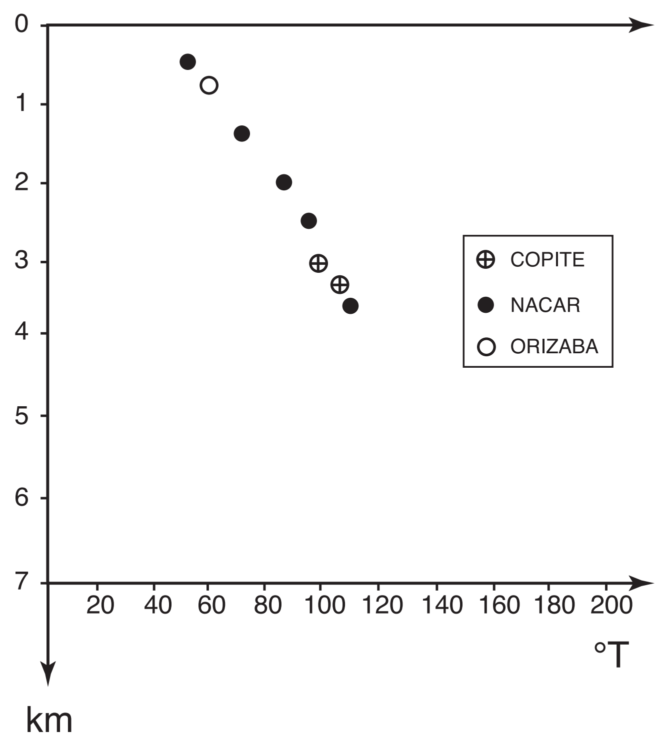

Figure 7. Bottom-hole temperatures (BHT) used for calibration of thermal models, with legend of the three boreholes used.

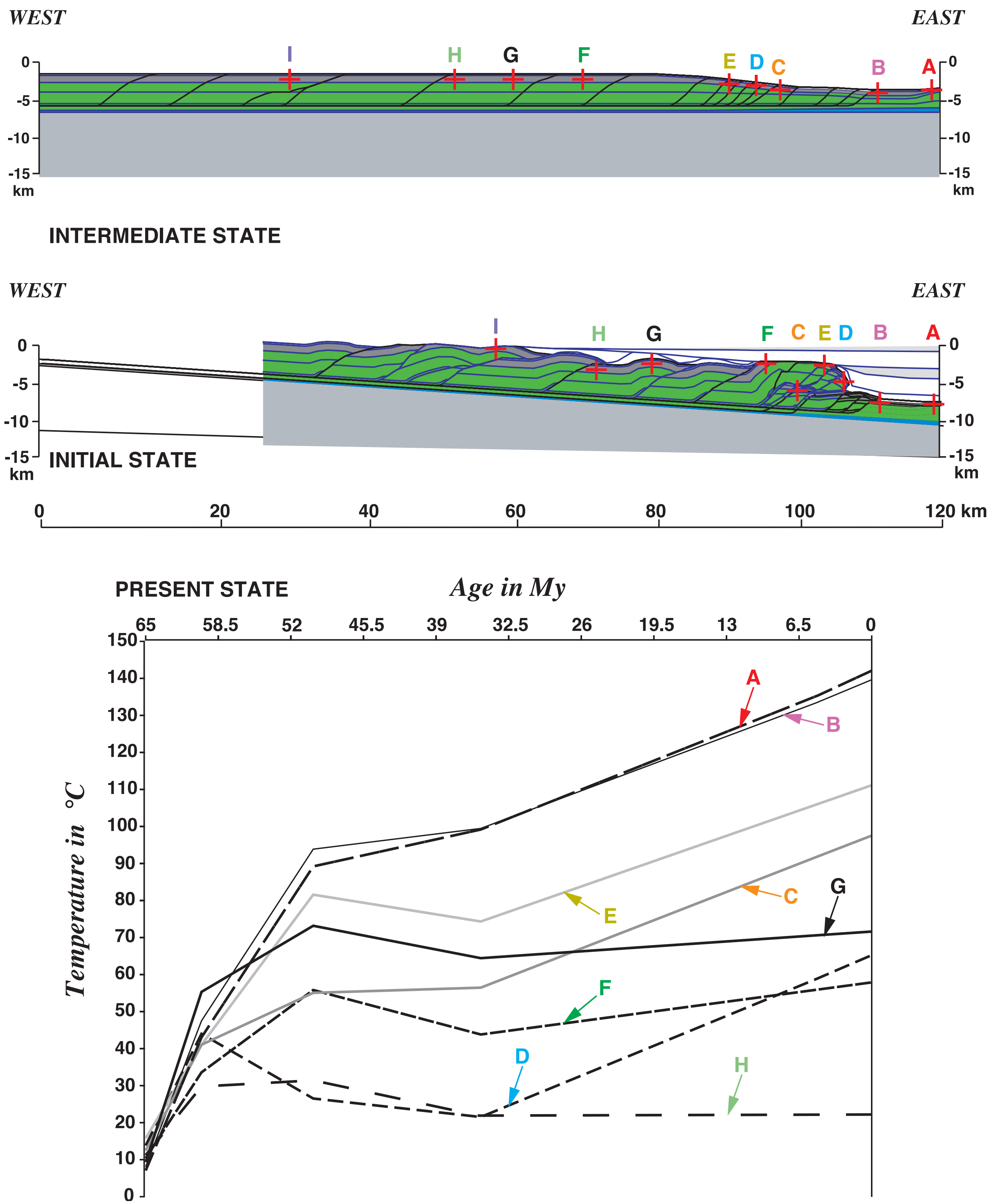

Figure 8. Result of the Thrustpack forward kinematic modeling for SUBTRAP northern transect I. Letters A through H represent control points used in modeling of temperature evolution across the Cordoba Platform as well as lines of temperature evolution.

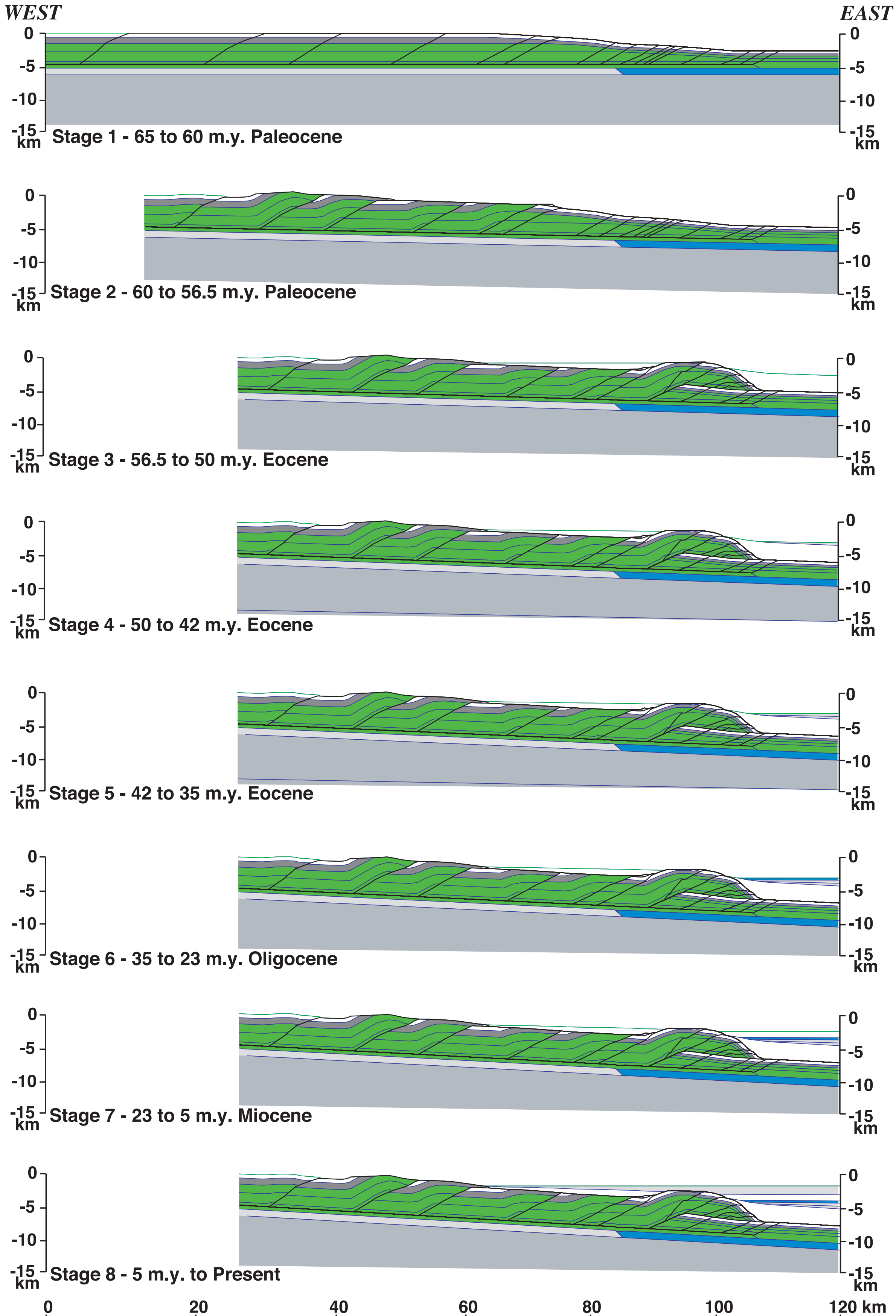

Figure 9. Results of the Thrustpack forward kinematic modeling for SUBTRAP central transect II.

Table 3. Distribution and characteristics of the main potential source rock intervals.

Stratigraphic age	*Kerogen type*	*TOC (average)*	*Distribution*
Upper Jurassic (Tepexilotla Formation)	II. Marine	0.4 to 0.5% (residual potential, in overmature outcrop samples)	Zongolica Basin (also in the Veracruz Basin?)
Lower Cretaceous (Tamaulipas Formation) (Neocomian-Aptian)	II. Marine		Zongolica Basin (Cordoba Platform?)
Middle Cretaceous (Orizaba Formation) (Albian-Cenomanian)	II. Marine		Orizaba and Cordoba Platforms?
Middle Cretaceous (Maltrata Formation) (Turonian)	II. Marine	3 to 4%	Eastern margin of the Cordoba Platform (also in the Veracruz Basin?)
Upper Cretaceous (San Felipe Formation) (Late Santonian-Campanian)	II. Marine		Eastern margin of the Cordoba Platform (also in the Veracruz Basin?)
Upper Cretaceous (Mendez Formation) (Maastrichtian)	II. Marine		Eastern margin of the Cordoba Platform (also in the Veracruz Basin?)
Paleocene (Velasco-Chicontepec Formation)	III. Terrestrial	5 to 6% (Mata Espino well)	Veracruz Basin

blanketing effect that contributed to a decrease of the geotherms.

Maturity Data of Potential Source Rock Horizons (T_{max} and R_o) and 1-D and 2-D Thermal and Petroleum Modeling of the Cordoba-Veracruz Transects

A number of R_o and T_{max} values used to calibrate Thrustpack modeling were measured and compiled by PEMEX-IMP in wells of the Cordoba Platform and adjacent Veracruz Basin (Ortuño, 1991; PEMEX-IMP, 1995). Additionally, new Rock-Eval measurements on a Late Cretaceous core of the Nido well and on Paleocene cuttings from the Mata Espino-101b well also were used for calibration (these new data may be requested from the principal author).

Preliminary 1-D Genex and Gentect thermal modeling was addressed in a discrete number of wells located either in the allochthon (Orizaba and Cordoba wells) near the thrust front or in the foreland autochthon of the Veracruz Basin (Figures 8, 9, and 10). Notice that these areas comprise very distinct paleogeographic domains, eventually developing very different heat flow histories as a result of past configuration of the lithosphere beneath the Orizaba Platform, the Cordoba Platform, and the Veracruz Basin. Unfortunately, the number of calibration points (R_o values) was too limited to provide accurate control or to document any clear heat-flow variations between these three paleogeographic domains. Another problem encountered relates to realistic estimates of the initial thickness of eroded series in both the Orizaba allochthon and the Cordoba Platform.

Subsequently, 2-D Thrustpack thermal modeling was carried out only on the Cordoba Platform, thus excluding the largest depocenters of the Veracruz Basin. As a result, the thermal simulation discussed below is restricted mainly to a single and homogeneous paleogeographic domain, with both lithospheric and crustal thicknesses considered constant through time. Consequently, the basal heat flow was held constant from one part of the section to the other and, thus, for the successive evolutionary episodes simulated with Thrustpack (Table 2). Assuming that the surface temperature was constant through time (i.e., 15°C), a heat-flow value of 30 $mW.m^{-2}$ is necessary at the base of the sediments in order to achieve a reasonable model and to fit available bottom-hole temperatures and the current distribution of the maturity data (T_{max} and R_o) (Figure 11).

Timing of the Petroleum Systems

The Thrustpack simulations were calibrated against the maturity data of potential source horizons, which were available mostly from surface outcrops and exploration wells located on structural highs. In contrast, these simulations also allow computation of the maturity evolution of potential source rocks in

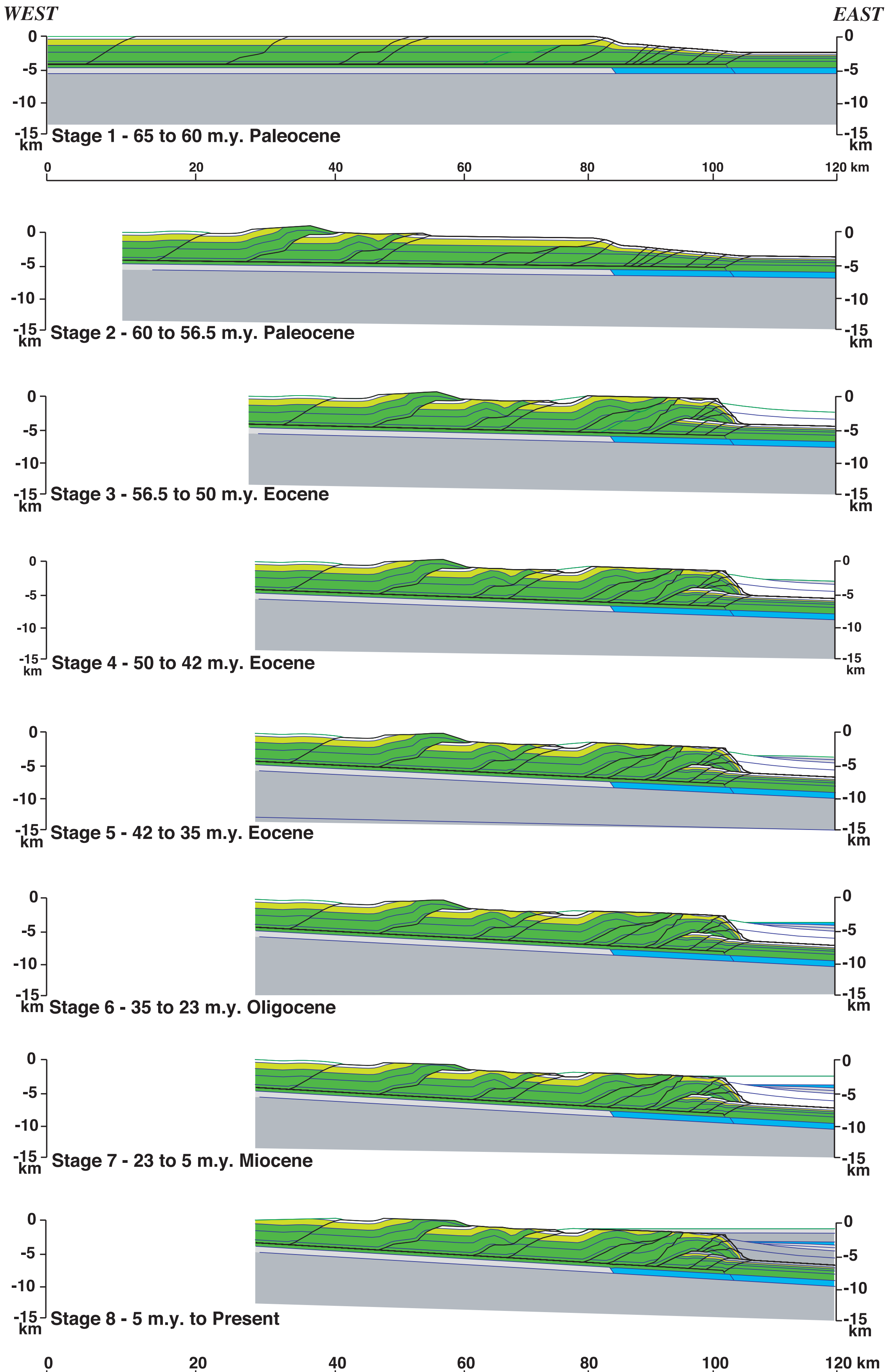

Figure 10. Results of the Thrustpack forward kinematic modeling for SUBTRAP southern transect III.

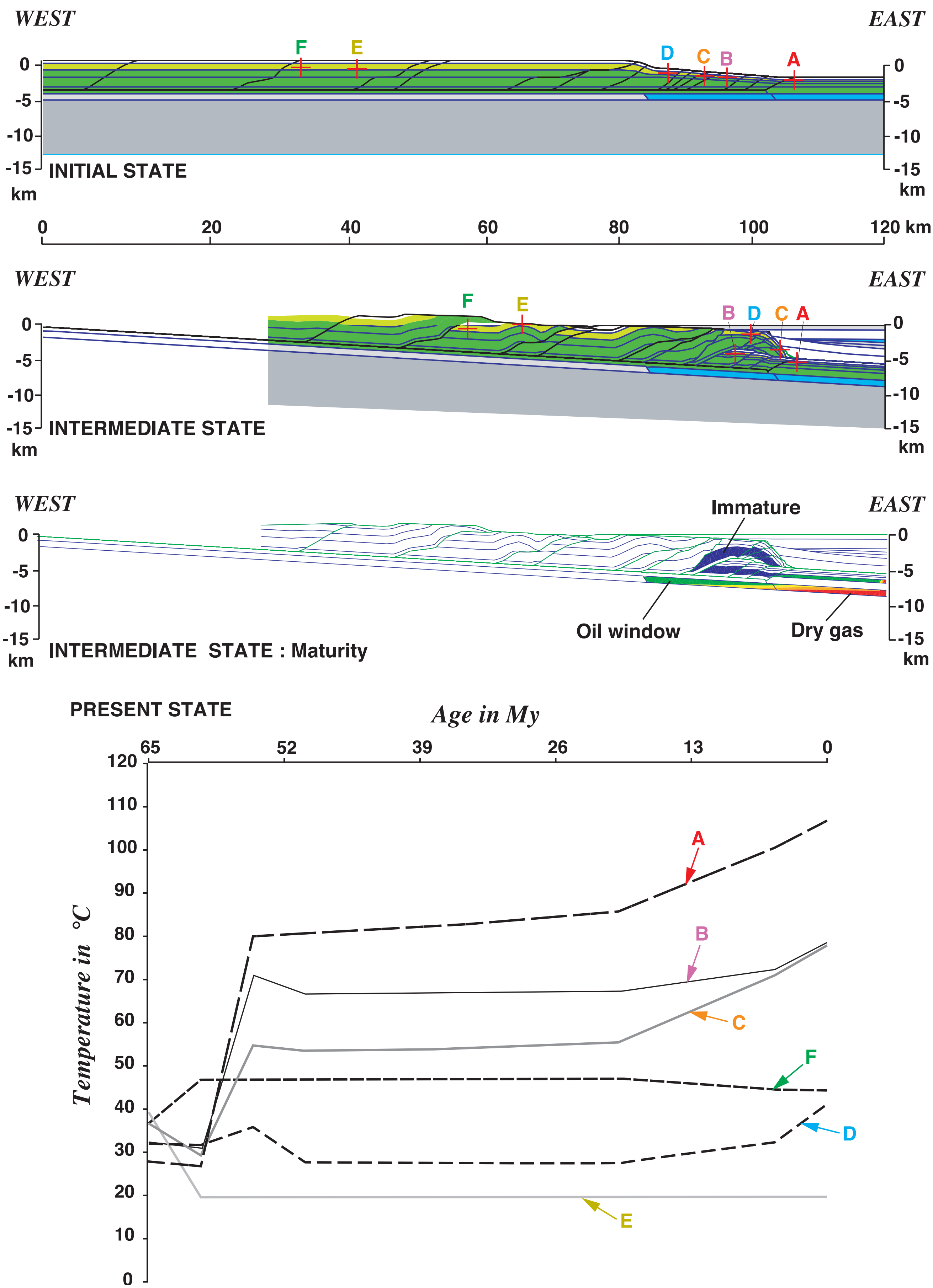
WEST
EAST
F
E
D
C
B
A
0
-5
-10
-15
km
INITIAL STATE
0
20
40
60
80
100
120 km
INTERMEDIATE STATE
Immature
Oil window
Dry gas
INTERMEDIATE STATE : Maturity
PRESENT STATE
Age in My
65
52
39
26
13
0
120
110
100
90
80
70
60
50
40
30
20
10
0
Temperature in °C

the intervening structural depressions, which likely constitute the active kitchens. However, because of contrasting paleogeographic environments, potential source rocks are not distributed equally across the Cordoba Platform: (1) For instance, Kimmeridgian source rocks are assumed to extend beneath the Veracruz Basin but are likely to disappear westward quickly where deep-marine settings are less developed. At the same time, it cannot be excluded that other nondeep-marine source rocks exist. (2) Seemingly, the Turonian organic-rich interval is well defined only in the vicinity of the platform-to-basin transition, but it is unlikely, according to available core and cutting data, that any major source-rock horizon occurs farther to the west in the Cordoba Platform. With this peculiar distribution of source-rock horizons and with results of the thermal modeling, it becomes evident that hydrocarbon accumulations discovered in the Late Cretaceous carbonate reservoirs of the buried Laramide thrust front are derived from a very recent kitchen (Figure 12). Thus, they developed in the footwall foreland and adjacent parts of the Veracruz Basin a long time after the foothill evolution. Tectonic burial was not yet sufficient during the Laramide orogeny to bring the potential source rocks of the Cordoba Platform and adjacent parts of the Veracruz Basin into the oil window. Unlike other segments of the Sierra Madre north of the volcanic axis where syn-Laramide trapping has been seen (Yurewicz et al., 1997), increasing Neogene burial in the Veracruz Basin is the dominant control for the distribution of the active kitchens in this part of Mexico.

This means that hydrocarbons have migrated both westward updip along the regional monocline and eventually upward through the basal décollement before reaching the frontal prospects. Alternatively, small kitchens also are likely to occur in the underthrust duplexes. However, carbonate reservoirs are no longer adequate for hydrocarbon storage when they have been breached by the post-Laramide unconformity. In this case, young hydrocarbons are likely to migrate updip along this unconformity, which indeed constitutes a regional conduit for fluid that either becomes biodegraded or remains trapped in stratigraphic traps involving Cenozoic sandstone reservoirs.

Oil seeps also have been locally recognized across the Cordoba Platform (i.e., in the Peñuela quarry: Ferket et al., 2003). Being located quite far west from the invoked eastern oil kitchens, two alternate hypotheses for these peculiar occurrences can be considered, namely:

1) short-range migration pathways from the nearby synclines (Figure 12). However, this hypothesis would require the occurrence of a hypothetical source-rock horizon in this part of the Cordoba Platform, eventually associated with the Lower Cretaceous evaporites. Unfortunately, this hypothesis could not be tested by geochemistry of the oils or by Lower Cretaceous source-rock extracts.
2) these accumulations are the result of a long-distance migration of early generated hydrocarbon from the west sourced by Kimmeridgian rocks of the Zongolica Basin when it was still part of the autochthonous foreland. It could thus have expelled hydrocarbons toward the east into the adjacent Cordoba Platform (Figure 12). This hypothesis also could not be tested by oil-source rock correlations, but this scenario is quite unlikely. Effectively, the current habitat of oil seeps relates to Laramide anticlines and, unless a remigration of early entrapped hydrocarbons occurred in individual thrust fold units, these oils successively should have crossed a number of thrust surfaces before reaching their current habitat.

Temperature Versus Depth Evolution of the Carbonate Reservoirs: Results from Thermal Modeling

The main result derived from thermal modeling with respect to the diagenetic history of the Late Cretaceous carbonate reservoirs relates to their temperature versus depth evolution. Successive paleotemperatures have been computed for each preselected reference point for the construction of burial curves, assuming purely conductive heat transfer (Figure 11).

These curves are representative of the foreland autochthon and buried duplexes of the Laramide thrust front and surface anticlines of the Cordoba

Figure 11. **Major results of the Thrustpack thermal and maturation modeling. Notice that oil kitchens are restricted to the Veracruz Basin and underthrusted foreland, and relate mostly to sedimentary burial beneath the post-Laramide sedimentary cover. Notice also that Late Cretaceous carbonate reservoirs of the Cordoba Platform located in ramp anticlines west of the Laramide thrust front always were preserved from deep burial and, thus, record maximum temperatures in the range of 60°C only.**

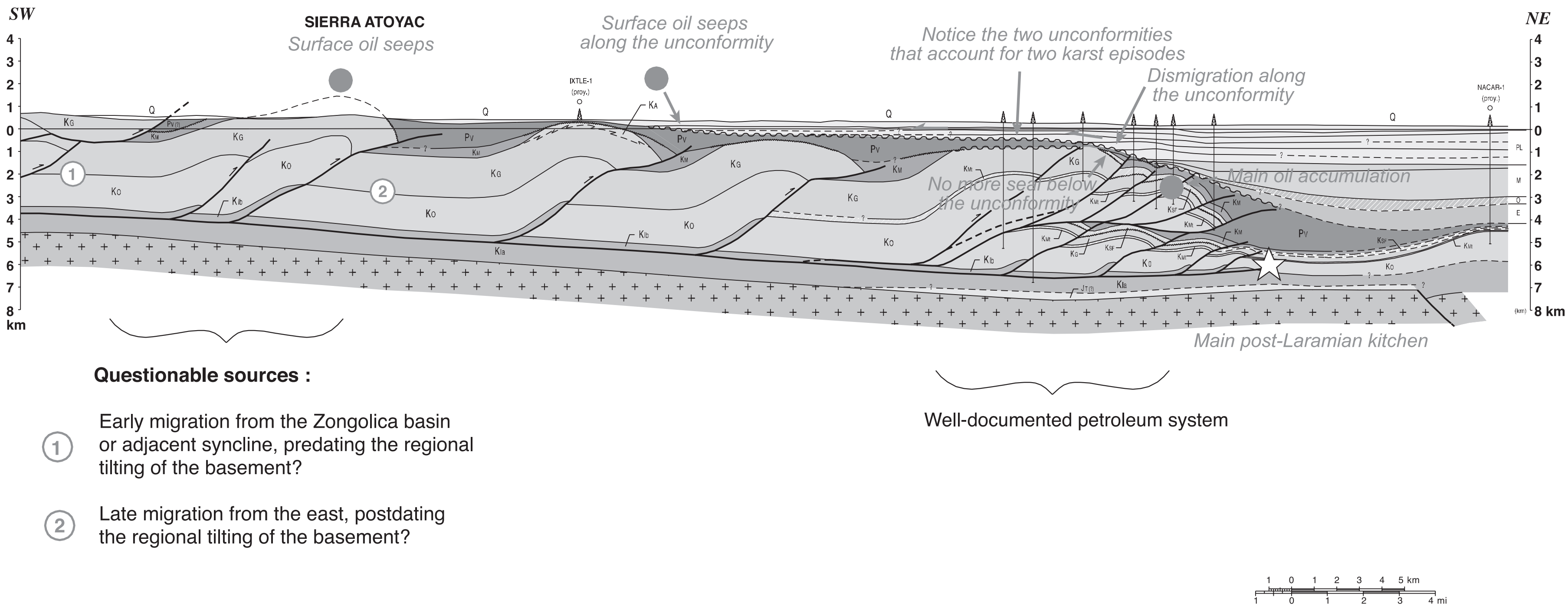

Figure 12. Potential migration pathways accounting for the present distribution of hydrocarbon accumulations and oil seeps in the buried duplexes of the Laramide thrust front and surface anticlines of the Cordoba Platform. Notice that oil migrated westward from the Veracruz Basin toward the Cordoba Platform, and that the post-Laramide unconformity is likely to act as a shallow conduit for oil where the Paleocene flysch (main seal) has been eroded.

Platform, respectively (Figures 2 and 12). As such, they allow the placement of individual diagenetic episodes into a more regional geodynamic and tectonic framework.

As already mentioned, burial of the Late Cretaceous reservoirs of the Cordoba Platform west of the Laramide thrust front appears always to have been limited, thereby accounting for maximum temperatures in the range of 60°C. In contrast, the deeper duplexes located in the buried thrust front reached their maximum burial and peak temperature only very recently, as a result of Cenozoic subsidence history of the Veracruz Basin.

Reservoir Potential

The productive fields are located mostly in the buried Laramide thrust front that developed along the eastern margin of the Cordoba Platform. As a result, the main middle to Late Cretaceous carbonate reservoir intervals display distinct paleogeographic affinities, from clear platformal paleoenvironments in the uppermost and westernmost units of the frontal triangle (i.e., the Albo-Cenomanian Orizaba Formation and part of the Turonian to Santonian Guzmantla Formation), to slope facies in the lowermost and easternmost duplexes (i.e., part of the Guzmantla Formation and the Campanian slope breccias of the San Felipe Formation).

Alternatively, Eocene and possibly Oligocene sandstone reservoirs occur also in the Veracruz Basin, as well as a few Miocene sandy horizons (i.e., the Chapopote Formation).

Reservoir-controlling Processes in Cretaceous Carbonates

The Guzmantla and Orizaba Formation reservoirs were studied both in outcrops and in wells along the regional transects at various distances from the thrust front. Reservoir porosity is characterized by both matrix and fracture porosity. A detailed diagenetic study of these formations, including transmitted light microscopy of stained thin sections, cathodoluminescence (CL), scanning electron microscopy (SEM), fluid inclusions, and stable isotopes revealed a succession of fluid-flow episodes during foreland evolution and deformation. This study allowed definition of the main reservoir-controlling factors (research in progress).

Crosscutting relationships among cementing phases, different stylolite sets, and fractures (e.g., Plate IIB) helped in reconstructing the paragenetic sequence of these reservoirs. Two types of stylolites can be differentiated, namely bed-parallel stylolites (BPS) forming horizontal stylolitic planes that relate to burial compaction, and layer-parallel shortening (LPS) stylolites, which are induced by tectonic shortening and develop perpendicular or oblique to bedding. The crosscutting relationships allowed differentiation of a pre-BPS early diagenetic burial history, a post-BPS but pre-LPS burial history, and a post-LPS history of syn- or postorogenetic fluid flow.

In this paper, attention is paid only to the principal regional reservoir controlling diagenetic processes, namely (1) matrix cementation and porosity preservation, (2) fracturing and hydro-fracturing, (3) karst formation, and (4) stylolite development.

Matrix Cementation and Primary Porosity Preservation

Primary porosity is often completely destroyed by early diagenetic cementation (Plate IIA); however, in some lithologies, primary porosity still is preserved (Plate IIB). Oil-impregnated lithologies of the Guzmantla Formation (Peñuela quarry and M.R. Aguilar-1A well) consist of finer-grained strata, whereas coarse bioclastic grainstones are not oil-impregnated despite their display of significant moldic macroporosity of telogenetic origin in the Peñuela Quarry (see below). Three main lithofacies can be differentiated; i.e., (1) bioclastic grainstones, (2) bioclastic wackestones to packstones, and (3) mudstones to wackestones. Bioclastic grainstones are characterized by early pore-occluding marine and meteoric cementation, which developed abundantly on ideal nucleation sites, such as crinoids, rudist fragments, etc. Isolated biomoldic pores exist but do not contribute to permeability, as attested to by these strata not being oil-impregnated. Mudstones to wackestones are marked by severe compaction that reduces both porosity and permeability. Oil-impregnation is limited to stylolitic planes (Plate IIH). The bioclastic wackestones to packstones also contain a number of sedimentary micrite allochems (e.g. peloids) as well as marine and meteoric cements that possess an appreciable (~15%), dominantly primary, porosity. Inter- and intraparticle (Plate IIB) as well as biomoldic pores are oil-impregnated. Here, cementation on nucleation sites such as crinoids and rudist fragments was less pervasive than in the grainstones, since these constituents are less common. This cementation did not occlude all primary pores, most likely since micrite constituents did not form good nucleation sites for cementation. This cement, however, created a stabilizing framework that protected the strata from compaction.

Plate II. **Overview of different photomicrographs displaying diagenetic features. (A) Photomicrographs of pervasively cemented peloidal grainstone (Guzmantla Formation); scale 1cm = 100 μm (Peñuela quarry). (B) Photomicrographs of partially cemented bioclastic wackestone with oil-stained primary interparticular and intraparticular porosity (brown colored)(Guzmantla Formation); scale 1cm = 100 μm (Peñuela quarry).**

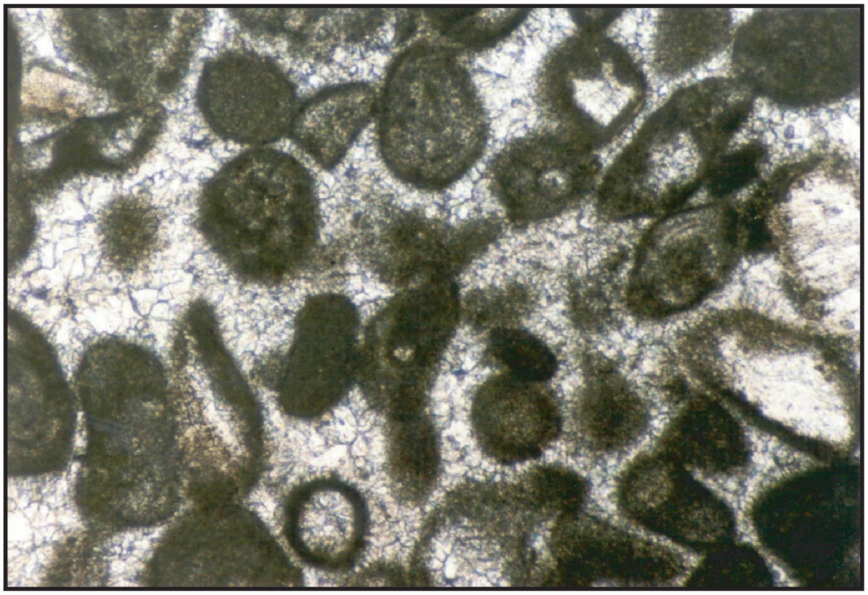

II A

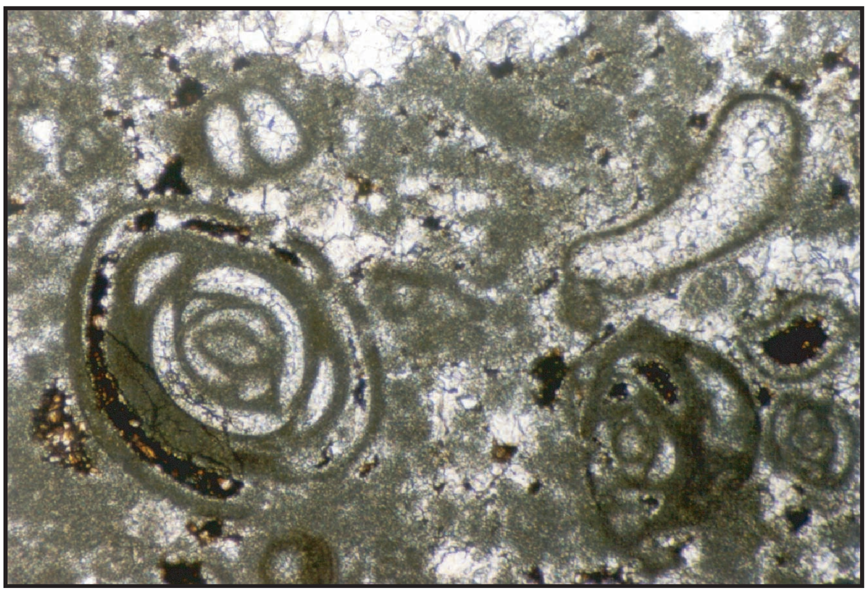

II B

After oil migration, telogenetic karst development preferentially affected the non oil-impregnated limestones of lithofacies 1 (bioclastic grainstones). However, oil did not migrate into these karst-related pores, most likely because of the oil's residual nature, the low overall temperature at the time of karst development and thereafter, the lack of driving forces.

These observations stress the important effect of sedimentary facies, and thereby paleoenvironments, on early diagenesis and porosity preservation (Ferket et al., 2003).

The Orizaba dolomites studied in the Tlacuiloltecatl area and in several wells in the eastern part of the study area possess good intercrystalline matrix porosity with some biomoldic and vugular porosity, thanks to early diagenetic dolomitization (Plate IB). Dolomitization by marine water or reflux of saline water is supported by the isotope data of these dolomites (see, for example, Figure 14), which are slightly enriched in ^{18}O compared to marine-derived Cretaceous constituents.

Fracturing and Hydrofracturing

Several fracture generations have been recognized whose petrographic characteristics and chemistry reflect an evolution in fluid characteristics during FFTB evolution (Ferket et al., 2003). The term ''hydrofracture'' is restricted here to fractures that are internally

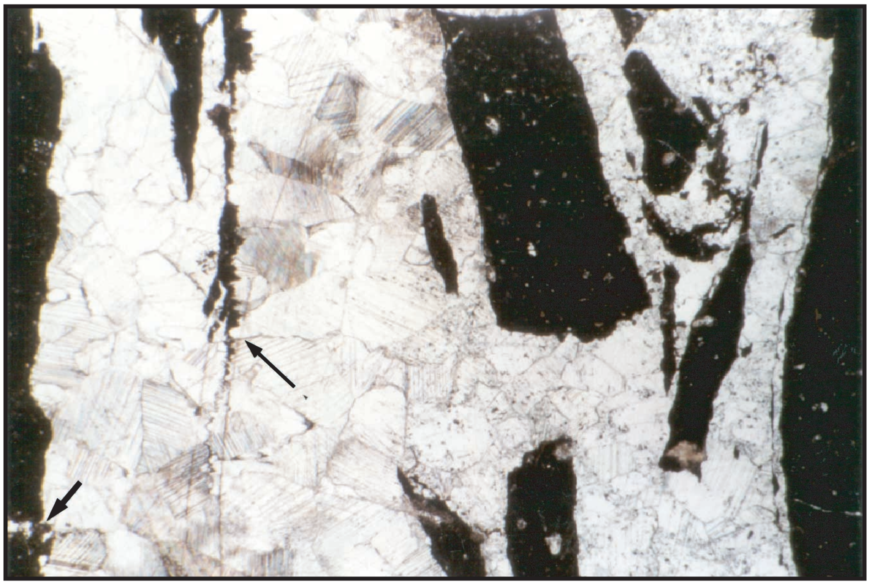

II C

Plate II. (cont.) (C) Photomicrographs of detail of a hydrofracture, with pieces of host-rock material floating in calcite cement. Notice that two different cement fabrics are present, testifying to the multistage development of these hydrofractures. Furthermore, an LPS sylolitic plane crosscuts the picture vertically (see arrow); scale 1cm = 625 μm. (D) Outcrop aspect of crack and seal fracture (Orizaba Formation; Vasquez Vela quarry); scale 1 cm = 1.3 cm.

II D

brecciated with pieces of host-rock material floating in the cement (Plate IIC and IIIA). These reflect overpressured regimes. Another type of fracture, the so-called crack and seal fractures (Plate IID), also reflect overpressures, since they document successive episodes of fluid pressure build-up and fracturing with concomitant pressure release and cementation. Both fracture systems most likely evolved into "classical" fractures cemented by one generation of calcite only.

Two major hydrofracture systems and several classical fracture systems have been differentiated.

An early (pre-BPS) set of hydrofractures (Plate IIE) is characterized by similar mineralogy, cathodoluminescence, and isotopic values as the host rock. The negative shift in oxygen isotopes of these veins and of the host rock with respect to the standard marine Cretaceous values (Figure 13) give evidence of precipitation from meteoric or modified fluids with precipitation at higher temperatures. Some veins with depleted $\delta^{18}O$ values (as much as $-13‰$ PDB) clearly reflect temperature-related fractionation (Figure 13). These fractures likely relate to early dewatering processes in a dominantly extensional regime.

A second set of hydraulic fractures (post-BPS but pre-LPS stylolite), which are mostly dipping at a high angle to bedding (Plate IIIB), display mineralogical, CL, and isotope characteristics that are similar to the host rock. In the Orizaba limestones and dolomites of the Tlacuiloltecatl area, however, these hydrofractures are filled with different mineralogies (saddle

Plate II. (cont.) (E) Cathodoluminescence photomicrograph of early set of (hydro)fractures displaying the same luminescence as the host rock. Notice that this fracture is cut by a BPS stylolite, which has been accentuated in black (Guzmantla Formation; Peñuela quarry); scale 1cm = 100 μm. (F) Cathodoluminescence photomicrographs of fractured, dull-brown luminescent dolomite host rock with crenulated, intensively zoned calcite cements with alternating bright-yellow to brown zones (Orizaba Formation; Nido 2 well); scale 1cm = 100 μm.

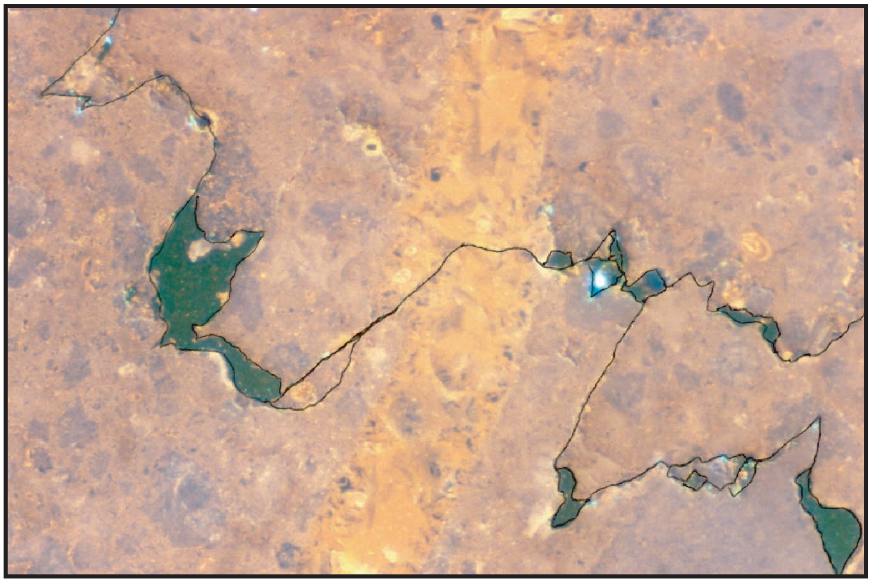

II E

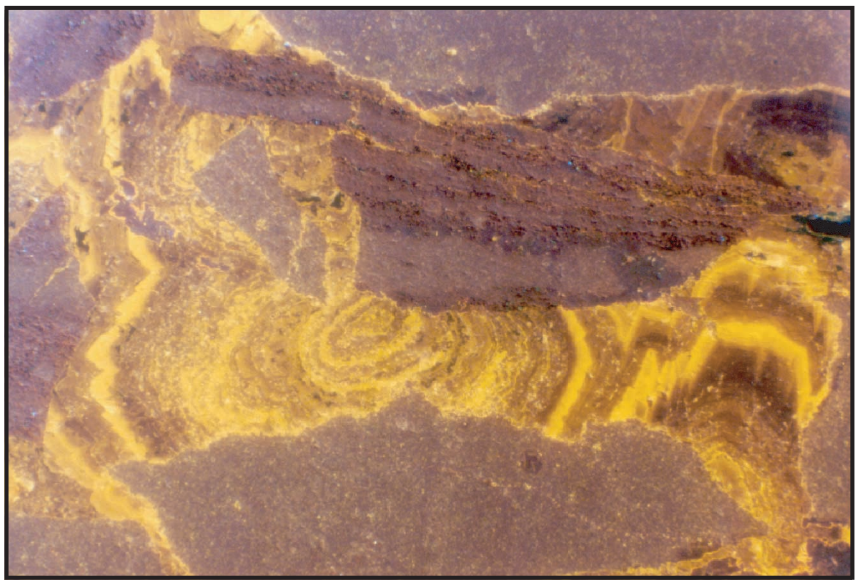

II F

dolomite in limestones, calcite-filled fractures in dolostone, fluorite) and, in the case of similar mineralogy as the host rock, display CL characteristics that differ from the host rock. The isotope values of several of the calcite fracture infilling show a trend towards depleted $\delta^{13}C$ values (as low as -10.5‰ PDB), reflecting cementation by karst-related fluids (Figure 14). The saddle dolomite and fluorite occurrences point towards involvement of hydrothermal fluids. All of these post-BPS and pre-LPS hydrofractures probably relate to the onset of regional tectonic contraction of the Laramide orogeny.

Although both hydrofracture generations currently are cemented and no longer contribute to fluid transfers, their existence demonstrates that overpressures might have preserved the reservoir to some degree from the effects of both vertical and horizontal compaction.

Post-LPS fractures in the western Cordoba Platform carbonates relate to the Laramide orogeny. Many of these fractures seem to have been reactivated during post-Laramide telogenetic time. The cements in the fractures reflect a meteoric isotopic signature and indications of soil-derived CO_2 ($\delta^{18}O$ values and $\delta^{13}C$ values varying, respectively, between -5.0 to -7.0‰ PDB, and +0.5 to -13.0‰ PDB).

Locally, as in the Orizaba dolomites of the Nido 2 well just above a major thrust fault, hydrofractures, some of which are clearly post-LPS, consist of a network of randomly oriented joints that evolved

II G

Plate II. (cont.) (G) Photomicrographs of pre-BPS karst and fracture system cut by a bed-parallel stylolite (accentuated in green color). Notice that some of the karst vugs are filled by a silt phase in which some foraminifera occur locally (Guzmantla Formation; Atoyac anticline); scale 1cm = 625 μm. (H) Photomicrographs of bioclastic to peloidal wackestone with oil-stained bed-parallel stylolite. (Guzmantla Formation; Atoyac anticline); scale 1cm = 625 μm.

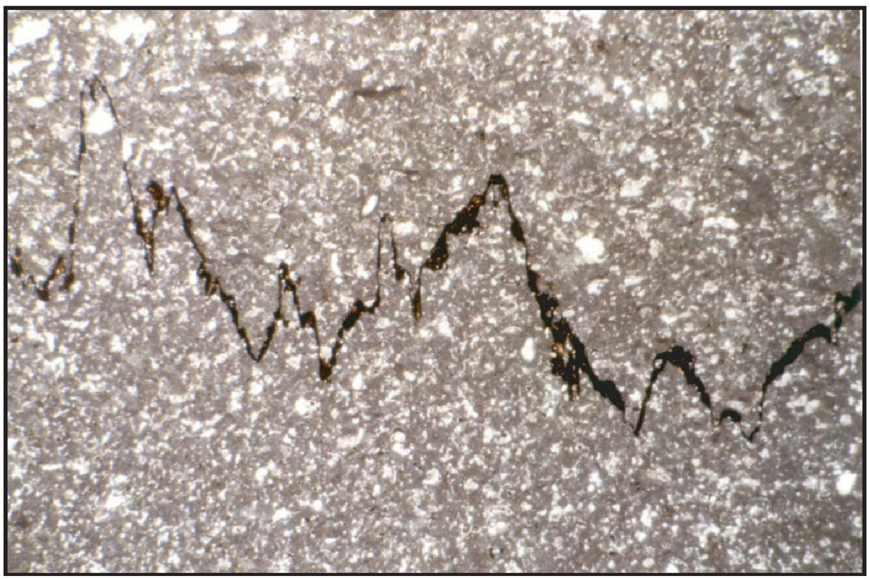

II H

locally into intensive brecciation of the dolomite. Some of these fractures were partially cemented by peculiar calcite cements with crenulated (Plate IIF), cauliflower, and feather CL patterns and shapes. Stable isotopes show very depleted $\delta^{13}C$ values (as low as -30‰ PDB, Figure 14), suggesting precipitation out of hydrocarbon-related fluids. The effect of this fracturing phase is of major importance for reservoir evolution, not only because permeability was enhanced strongly, but also since the seal can be damaged. The cements are interpreted to be bacterially mediated. Infiltration of bacteria is explained by Orizaba dolomites being situated near the Nido 2 well location, close to an exposure surface during the Oligocene-Miocene (post-LPS). The very negative $\delta^{13}C$ signatures are assumed here to relate to CO_2 produced during the biodegradation of migrating hydrocarbons. Indeed, Thrustpack modeling places oil migration within this time framework. The interplay of several time-related processes— i.e., thrust emplacement in the tectonic front position, hydrofracturing near a major fault zone due to fluid expulsion, oil maturation, and the near-surface position of the dolomite— gave rise to these peculiar calcite cements. Vertical escape of compaction fluids usually occurs in the vicinity of major normal faults in most passive-margin and foreland settings (Sassi and Faure, 1997).

Other microstructures that are of interest are: (1) conjugate high-angle strike-slip faults with evidence of pressure-solution and slickenside lineations mostly

Plate III. (A) Photomicrograph of pre-BPS hydrofracture in strata of the Guzmantla Formation of the Atoyac anticline; scale 1cm = 625 μm. (B) Outcrop image showing set of vertical, thick hydrofractures (notice the floating brecciated host-rock fragments) cut by a set of inclined to horizontally oriented thin calcite fractures. The arrow indicates the top of the sequence. The circles are the places where cores have been taken for petrographic analysis (Tlacuiloltecatl Anticline).

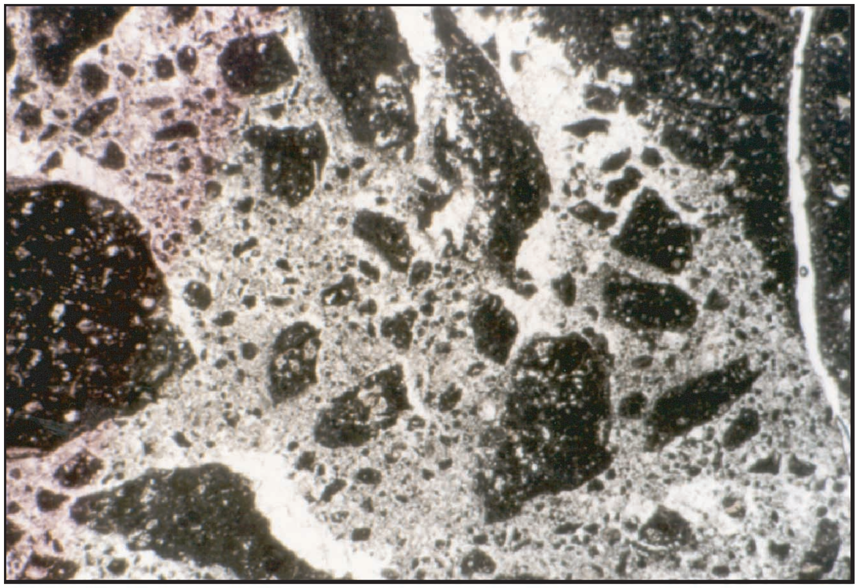

III A

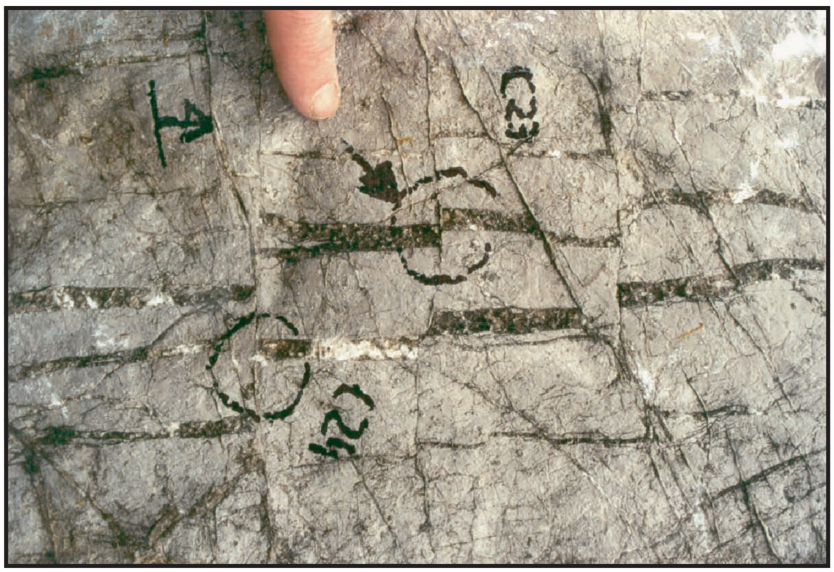

III B

parallel to the bedding that relate to incipient LPS. They predate the folding episodes (Plate IIIC and D); and (2) open joints perpendicular to the bedding, which are likely to relate to syn-folding extrados structures and which constitute the dominant set of microstructures, for example in the Peñuela quarry (Plate IIIE).

Although most fractures are cemented during FFTB evolution, reopening of some fractures during folding and the use of older fractures by later karst-related fluids is a common phenomenon and stresses the important control that fractures may exert on reservoir performance. It is noteworthy that the fracturing style is lithologically controlled. A well-defined system of straight, preferentially oriented fractures develops in limestones, whereas these fractures in dolomites are more dispersed and of brecciation type. Nonetheless, the most important set of microstructures accounting for secondary porosity and permeability in the Late Cretaceous carbonates of the Cordoba Platform seems to relate to extrado fractures, at least in the Peñuela quarry, which is one of the best large and unweathered outcrops allowing 3-D observations (Plate IIIE).

Karst Development

At least two episodes of karstification have been recognized in the western part of the platform. Here, thrust sheets remained at a relatively shallow position during foreland evolution, as deduced from Thrustpack modeling. Only in the east were Cretaceous

Plate III. (cont.) (C and D) Outcrop view of bed with conjugated faults (for detail, see D) (Tlaculoltecatl Anticline).

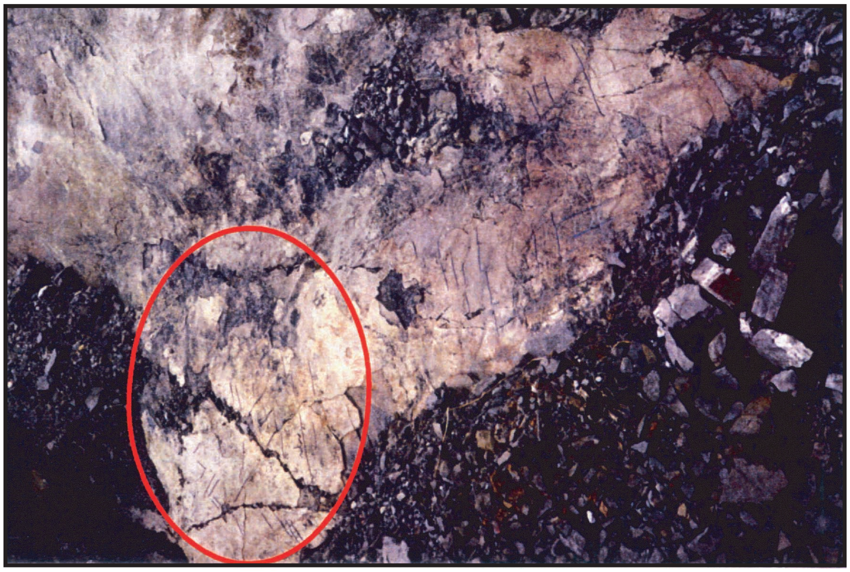

III C

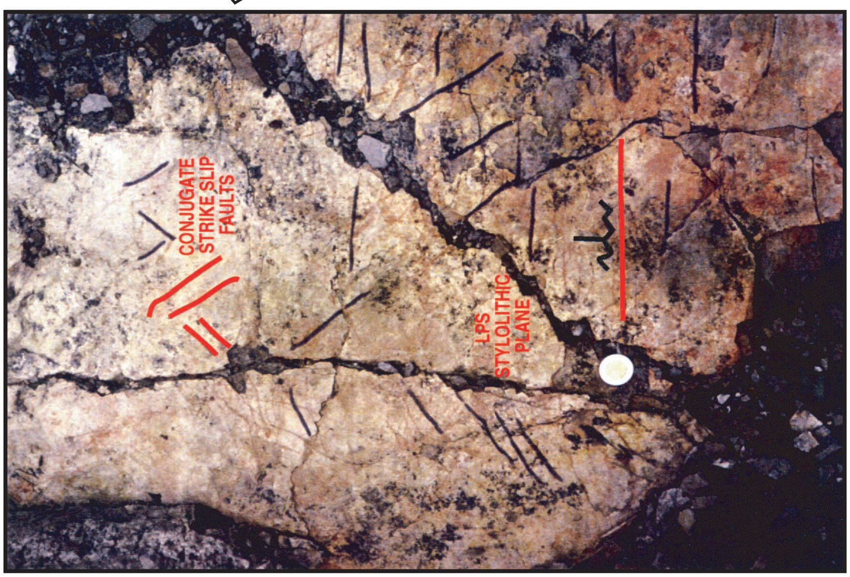

III D

carbonates deeply buried beneath the Veracruz Basin, as a result of Tertiary subsidence of the basin.

A pre-BPS karst system (Plate IIG) was observed only in the Atoyac area relating to a pre-BPS emergence phase (late Campanian) . During the late Campanian, onset of tectonic contraction occurred in the western hinterland while slope breccias of the San Felipe Formation were deposited along the eastern border of the Cordoba Platform. The early local karstification is interpreted, therefore, to relate to early flexural bulge development.

Telogenetic karst development is represented all over the western Cordoba Platform by dissolution and cementation, especially along fractures. Hydrofractures with silt infill also have been recognized in the eastern buried front (e.g., the Nido well). These relate to a karst episode in this area, caused by meteoric water infiltration derived from the paleokarstic surfaces that formed before onlapping of Tertiary strata from the nearby subsiding Veracruz Basin.

Karst-related cavities in the Peñuela quarry were not filled with oil, most likely because of the residual nature of the oil. However, in similar features in time-equivalent strata of the M.R. Aguilar-1A well, post-LPS dissolution vugs are filled with oil.

Stylolite Development

As mentioned before, two types of stylolites can be recognized; namely, bed-parallel stylolitic planes (BPS), which are best developed in massive carbonate

Plate III. (cont.) (E) Outcrop view of alternation oil- (black) and nonoil- (white) stained bed in the Peñuela quarry with clear development of open vertical extrados fractures; field of view, 20 by 14 m. (F) Outcrop view of massive limestone with black chert nodules and bed-parallel stylolites (Atoyac anticline).

III E

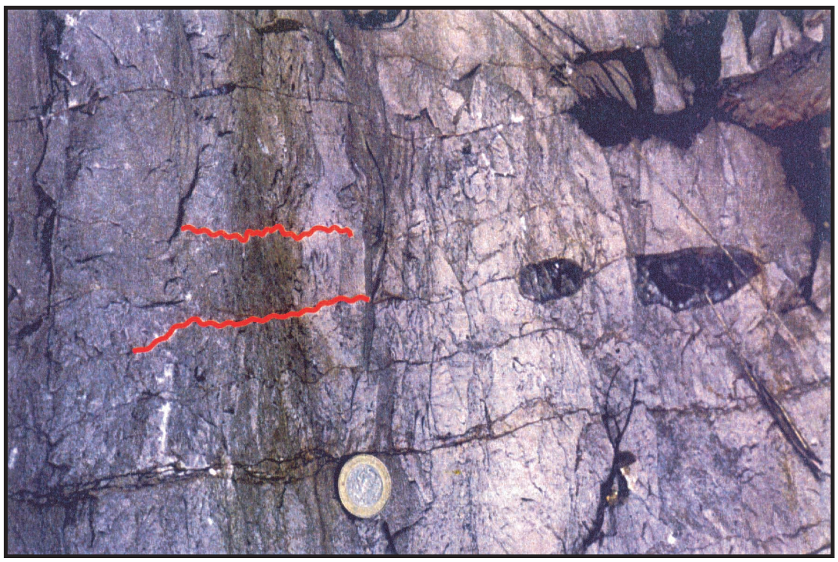

III F

sequences devoid of any major shaly interbeds (Plate IIIF), and stylolitic planes perpendicular to the bedding and coeval with orthogonal tension joints. The latter also account for prefolding LPS deformation (Plate IIIG and H). LPS stylolitic planes develop immediately prior to thrust emplacement (Averbuch et al., 1992; Frizon de Lamotte et al., 1997). Stylolites originally form permeability barriers, since they reflect pressure dissolution. However, in the Cordoba Platform, bedding-parallel stylolitic planes are not cemented and commonly are the site of secondary porosity development. As they are often oil-stained (Plate IIH), they still can act as potential conduits for horizontal fluid transfers. Seemingly, stylolitic planes perpendicular to the bedding often are cemented and thus useless for present fluid flow and hydrocarbon storage. However, fluid flow along these planes occurred in the past. In folded areas, LPS joints were selectively reactivated and reopened during subsequent folding episodes, and they account for secondary porosity, thus contributing again as potential conduits for fluids. Similar features have been documented by Van Geet et al. (Personal Communication, 2002) from Cretaceous carbonate reservoir strata in the Albanian Foreland Fold and Thrust Belt.

Spatial Distribution of Structural Features and Microstructures

In Figures 15 and 16, a synthesis is given on the general geometrical relationships and orientation of the deformation patterns, as well as a conceptual 3-D model of the structural pattern of the tectonic front.

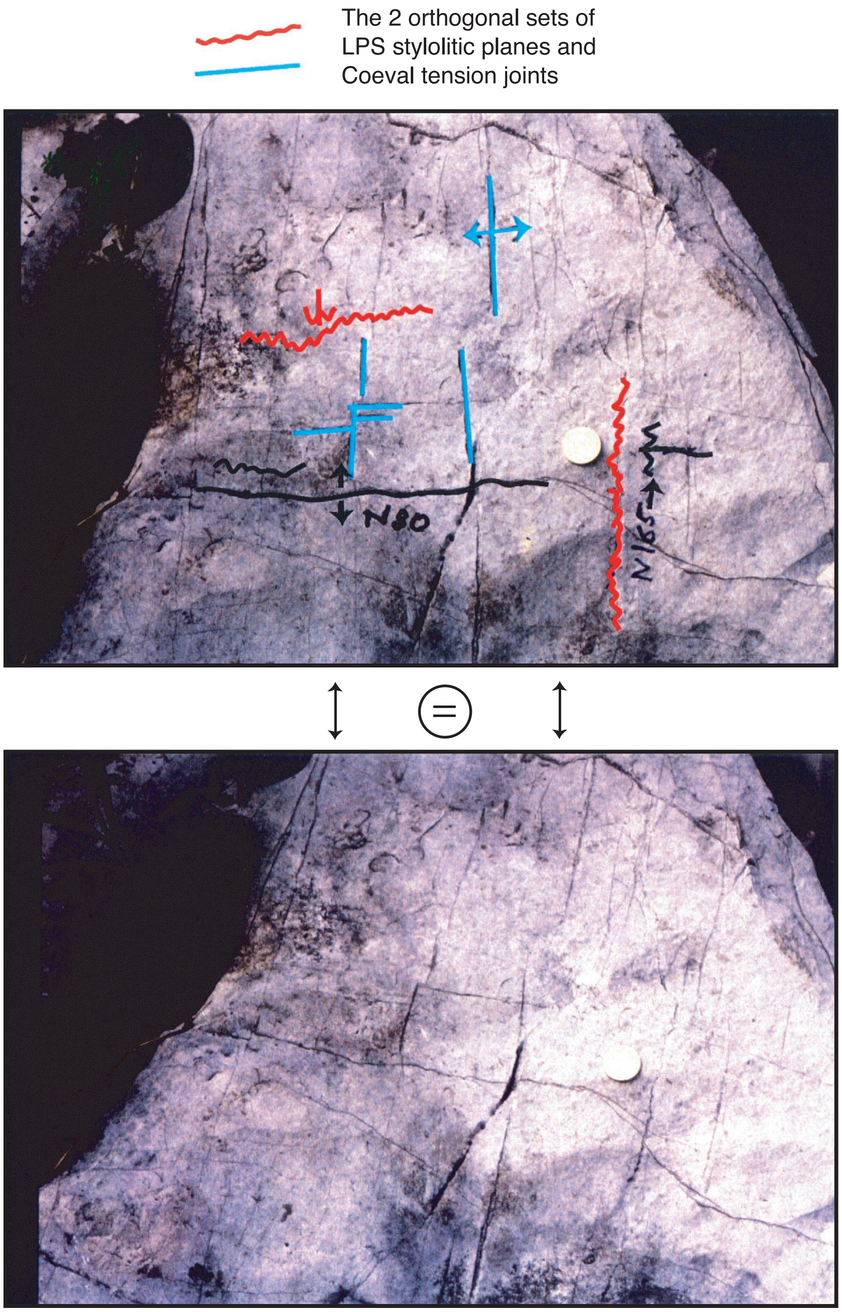

III G

III H

Plate III. (cont.) (G and H) Outcrop and interpreted outcrop pictures showing the development of two orthogonal sets of LPS stylolitic planes and coeval tension joints (Atoyac anticline).

This synthesis relies on field observations west of the buried front zone, as well as on a regional teledetection study conducted by Ortuño (1991).

The direction of the tectonic vector is generally NE 50–60° SW, while those of the folded structures are in general NW 30–40° SE. The variation in orientation is mainly because of sectors of the Sierra Madre Oriental where the structures turn slightly to the south (Figure 1) and, consequently, where the kinematic feature orientations also change slightly.

The fracture pattern is more diverse in orientation, with the most important fracture systems trending in the following directions: NE 45° SW, NE 5° SW, and NW 65–50° SE. These systems correspond to fractures and crosscutting vertical-to-subvertical systems that relate to compressional deformation. Planes varying around a NW 45° SE direction can be deduced from the data shown in Figure 16. These planes, which trend more or less parallel to the fold axes, relate either to LPS stylolitic planes inherited from the foreland evolution, or to extrados fractures, part of which eventually result from the reactivation of LPS joints during the folding episodes. Superimposed on these systems is the manifestation of conjugate fractures,

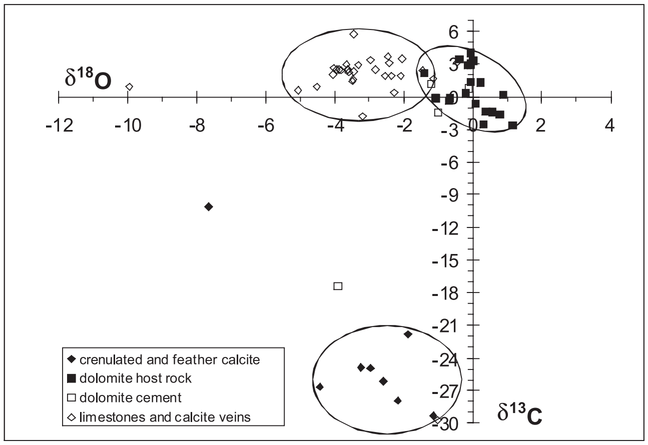

Figure 13. Stable isotope crossplot of diagenetic phases in the Atoyac anticline. The small gray rectangle indicates the marine calcite signature in equilibrium with Cretaceous seawater (based on Czerniakowski et al., 1984; Swennen and Dusar, 1997; Frank and Arthur, 1999).

which locally seem to cut some of the principal compressive systems. These systems might play a major role in the compartmentalization of the reservoirs.

It is stressed again that of all these structures, those that occur in extrados zones present the best conditions for reservoir development, since often they are open. They consist mainly of extrados fractures generated by extension and by reactivated LPS planes and fracture systems with a general northeast-southwest direction. These systems, which crosscut the entire Cretaceous carbonate section, form structures characterized by effective secondary porosity, along which vertical fluid circulation can occur.

CONCLUSIONS AND PERSPECTIVES

The main results of this SUBTRAP Mexican integrated study relate to the evolution of the rock matrix of carbonate reservoirs and its relationship to fracture and stylolite systems, and also to the general state of the petroleum systems:

- Potential source rocks are located mainly along the eastern margin of the Cordoba Platform and in the adjacent Veracruz Basin. However, they did not reach the oil window prior to the post-Laramide episodes of burial. This means that hydrocarbons essentially migrated westward and upward from the Veracruz Basin, and the underthrust foreland migrated toward the productive duplexes of the buried Laramide thrust front, thus significantly postdating the end of the main contractional episodes.
- According to Thrustpack simulations, the maximum temperature reached in the Late Cretaceous reservoirs of the Cordoba Platform west of the Laramide deformation front probably never exceeded 60°C. This is also attested to by the monophasic nature of the fluid inclusions and agrees with the low maturity rates recorded by organic matter.
- In contrast, the deeper duplexes located in the buried thrust front reached their maximum burial and peak temperature only very recently as a result of Cenozoic subsidence of the Veracruz Basin.
- The paleoenvironment accounts for preservation of reasonably good matrix porosity in distinct lithofacies (i.e., in early dolomitized platform carbonates of the Orizaba and Guzmantla Formations, in bioclastic wackestones to packstones in the Guzmantla Formation, and in slope breccias of the San Felipe Formation).
- Early episodes of hydraulic fracturing have been documented locally. In some samples from the Atoyac anticline, hydraulic fractures predate the bedding-parallel stylolitic planes and likely relate to early dewatering along vertical conduits in a dominantly extensional regime. A second episode of hydrofractures now is cemented by karst-related fluids, but some infill with saddle dolomite and fluorite also support the involvement of hydrothermal fluids. These hydrofractures probably relate to the onset of regional Laramide contraction. Elsewhere (i.e., in the Nido well), hydraulic fractures postdating LPS features occur, and are partially cemented by bacterially derived calcite caused by the biodegradation of

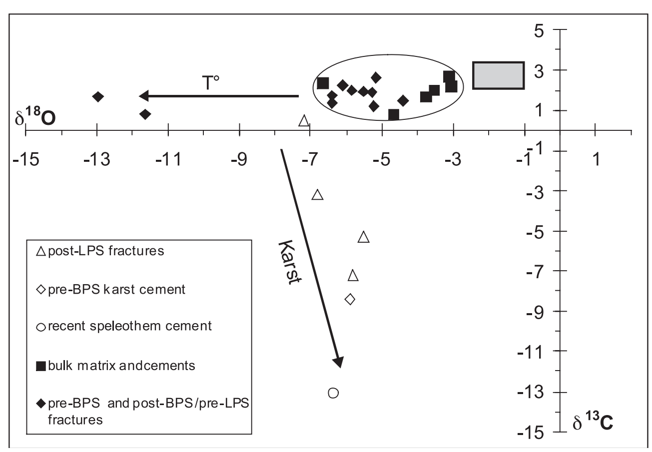

Figure 14. Stable isotope crossplot of diagenetic phases in the Nido 2 well. For reference to the calcite signature in equilibrium with Cretaceous seawater, see Figure 13.

Structure type	Cordoba Platform		
σ1	NE 50–60°SW		
Fold axes	NW 30–40°SE		
Fractures	Compression		
	NE 45° SW	NW 30° SE	NW 86° SE
	NE 70° SW	NW 10° SE	NW 80° SE
	NE 05° SW	NW 65° SE	NW 70° SE
	NE 30° SW	NW 15° SE	
	NE 85° SW	NW 45° SE	
	NE 65° SW	NW 25° SE	
	≈ E - W		
LPS	Compression	Compression Transtension	Others
	NW 45° SE	NW 65° SE	NE 70° SW
	NW 52° SE	NW 85° SE	≈ N - S
Conjugate faults	Compression - Transtension		
	NE 35°–55° SW; NE 60°–80° SW — Regional attitude		

High-angle faults and fractures

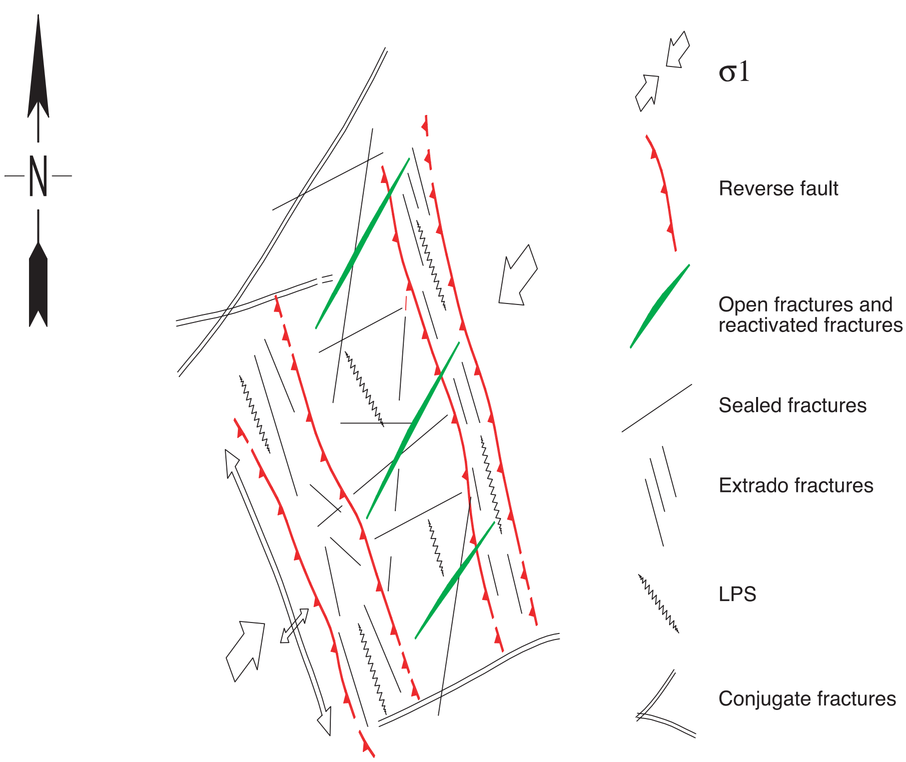

Figure 15. Data on dominant orientations of high angle faults and fractures of the Cordoba Platform with structural sketch and distribution of the fracture systems, faults, LPS joints, and other structures in the rocks. See Figure 1 for location.

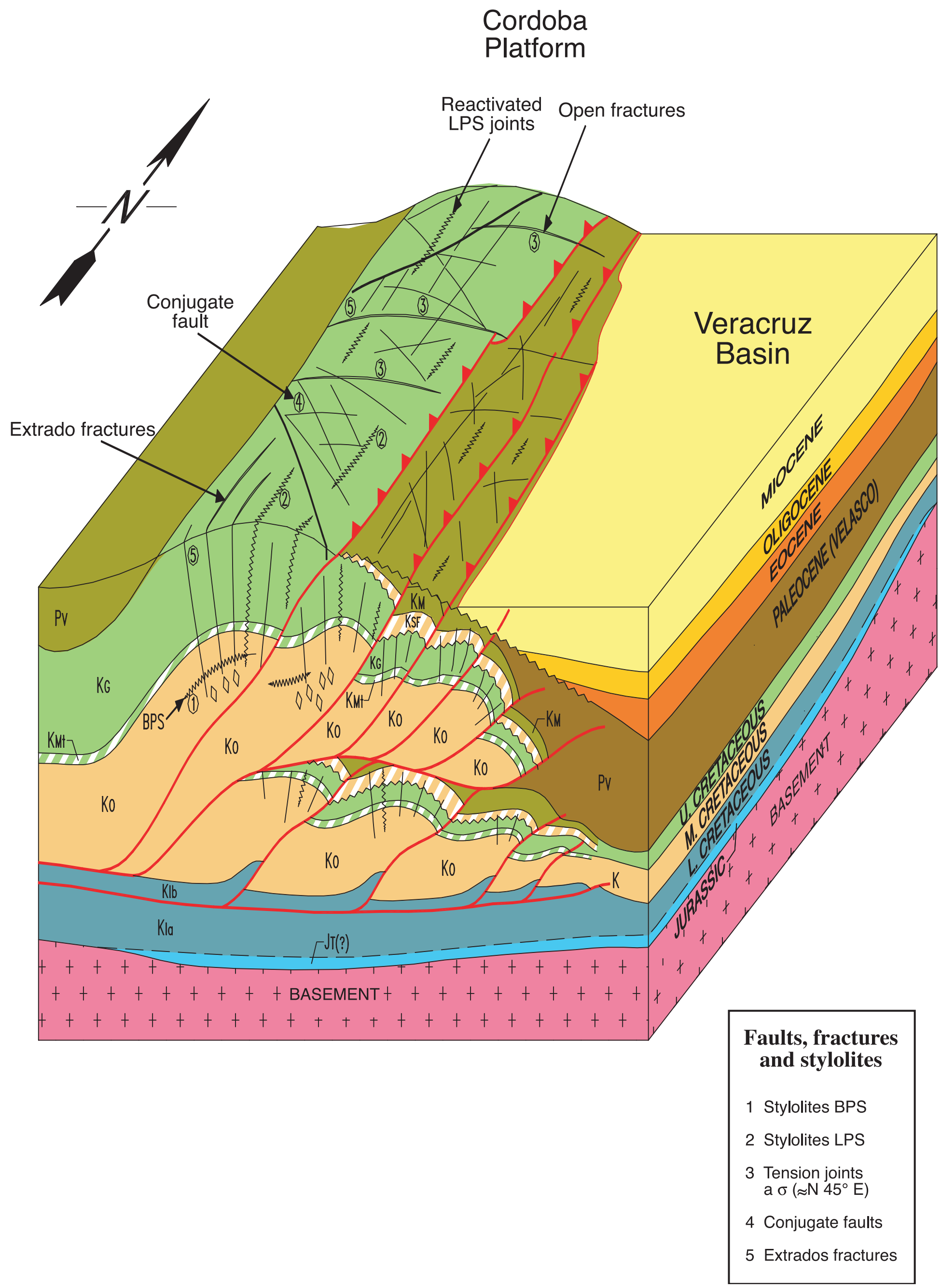

Figure 16. Block diagram outlining the thrust architecture and distribution of fractures and other microstructures near the thrust front. (J = Jurassic; K = Cretaceous; K_l = Lower Cretaceous; K_O = Orizaba Formation; K_{Mt} = Maltrata Formation; K_G = Guzmantla Formation; K_{SF} = San Felipe Formation; K_M = Mendez Formation; P_V = Paleocene Velasco Formation).

hydrocarbons. This type of hydrofracturing is recognized at different places adjacent to major faults. This open fracture network clearly improves reservoir permeability, but it may also locally damage the seal and cause these areas to leak. The second set of hydraulic fractures was mostly synchronous with the onset of the Laramide orogeny and occurred when the principal stress axis (σ_1) was already horizontal.

- Deformation features created secondary porosity during the Laramide orogeny. These Laramide microstructures comprise stylolitic planes perpendicular to the bedding, which result from pressure solution during episodes of layer-parallel shortening (LPS) and from tension joints parallel to the transport direction. These microstructures developed when the carbonate reservoirs still were attached to the autochthonous foreland; thus, they frequently are cemented still. However, portions of these planes were selectively reactivated and reopened during subsequent episodes of folding. Therefore, stylolitic planes caused LPS and orthogonal joints still act locally as vertical conduits for the fluids and display fair to good porosity and permeability characteristics, especially in the extrados and near-lateral anticlinal closures, or at places where their overall orientation is consistent with the post-Laramide (modern) stress pattern.

- Other carbonate cements in the Nido-2 well were caused by late interactions of the reservoirs with meteoric water, which occurred synchronously with the entrapment of the hydrocarbons and in association with bacterial activities (telogenetic karst development). Alternatively, the most important factor controlling the development of secondary porosity in the Cordoba Platform carbonates appears to relate to two successive karstification episodes. The first episode was related either to global sea-level changes during the passive-margin evolution or to the early development of a former Laramide flexural bulge. The second episode postdated Laramide contraction.

ACKNOWLEDGMENTS

This work benefited greatly from the technical assistance of PEMEX and IMP. Guillermo Perez and Noel Holguin provided all the support and enthusiasm necessary to organize the PEMEX-SUBTRAP-IFP field seminar in Veracruz and Cordoba, and initiated this international collaboration. The University of Cergy (Dominique Frizon de Lamotte) provided drilling tools for collecting oriented plugs in the field. Dominique Guérillot (IFP), Ricardo Caraveo, and Miguel Espinoza (PEMEX) also participated in the field work. Ricardo Caraveo and Miguel Espinoza, together with Modesto Landeros, also were very helpful in collecting core samples in Veracruz. Francine Bénard handled preliminary runs of Genex and Gentect on some of the wells. Herman Nijs prepared all the thin sections. We also would like to thank Chris Johnson and an anonymous reviewer for their helpful suggestions on an earlier draft of this paper.

REFERENCES CITED

Anderson, T. H., and V. A. Schmidt, 1983, The evolution of Middle America and the Gulf of Mexico–Caribbean Sea during Mesozoic time: Geological Society of America Bulletin, v. 94, p. 941–966.

Anderson, T. H., and L. T. Silver, 1974, Late Cretaceous plutonism in Sonora, Mexico, and its relationship to Circum-Pacific magmatism (Abs.): Geological Society of America, Abs., v. 6, p. 484.

Armstrong, R. L., 1974, Magmatism, orogenic timing and orogenic diachronism in the Cordillera from Mexico to Canada: Nature, v. 247, p. 348–351.

Aubouin, J., R. Blanchet, J. F. Stéphan, and M. Tardy, 1977, Téthys (Mésogée) et Atlantique: Conseil de la Recherche Académie des Sciences, Paris, France, 285(D), p. 1025–1028.

Aubouin, J., J. Debelmas, and M. Latreille, 1980, Les chaines alpines issues de la Téthys. Introduction générale, *in* Géologie des chaines alpines issues de la Téthys: Mémoires Bureau des Recherches Géologiques et Minières, Orléans, no. 115.

Averbuch, O., D. Frizon de Lamotte, and C. Kissel, 1992, Magnetic fabric as a structural indicator of the deformation path within a fold-thrust structure: A test case from the Corbieres (NE Pyrenees, France): Journal of Structural Geology, v. 14, p. 461–474.

Buffler, R. T., and D. S. Sawyer, 1985, Distribution of crust and early history, Gulf of Mexico Basin: Gulf Coast Association of Geological Societies Transactions, v. 35, p. 333–344.

Burkart, B., and C. R. Scotese, 1992, Orizaba fault zone of the western isthmus of Tehuantepec, Mexico: Delineation of the western margin of the Yucatan (Maya) block, in Mesozoic and early Cenozoic development of the Gulf of Mexico and Caribbean region (Abs.): 13th Annual Research Conference, Houston, Gulf Coast Section, Society for Sedimentary Geology (SEPM), p. 11–12.

Burke, K., C. Cooper, J. F. Dewey, P. Mann, and J. L. Pindell, 1984, Caribbean tectonics and relative plate motions: Geological Society of America Memoir 162, p. 31–63.

Campa, M. F., and P. V. Coney, 1983, Tectonostratigraphic terranes and mineral resource distribution in Mexico: Canadian Journal of Earth Sciences, v. 20, p. 1040–1051.

Campa, M. F., M. Campos, R. L. Flores, and R. Oviedo, 1974. La secuencia mesozoica volcánica–sedimentaria metamorfizada de Ixtapan de la Sal, Mex. Teloloapan, Gro.: Boletín de la Sociedad Geológica Mexicana, v. 35, p. 7–28.

Carrasco, B., 1978, Estratigrafía de unas Lavas Almohadilladas y Rocas Sedimentarias del Cretácico Inferior en Tehuacán, Pue. Nota Técnica: Revista Instituto Mexicano del Petroleo, v. 7, no. 4, p. 7–27.

Carfantan, J. C., 1986, Du système cordillérain nord-américain au domaine caraïbe; étude géologique du Mexique méridional: Ph.D. Thesis, University of Chambéry, France, 558 p.

Coney, P. J., 1978, Mesozoic-Cenozoic Cordilleran plate tectonics: Geological Society of America Memoir 152, p. 33–50.

Córdoba, D. A., M. Tardy, J. C. Carfantan, M. F. Campa, and C. Rangin, 1980, Le Mexique mésogéen et le passage du système cordillérain de type Californie: 20th Congrès International, Paris, Colloque C.5, p. 18–29.

Cruz-Helu, P., V. R. Verdugo, and P. R. Barcenas, 1977, Origin and distribution of Tertiary conglomerates, Veracruz Basin, Mexico: AAPG Bulletin, v. 61, p. 207–226.

Czerniakowski, L. A., K. C. Lohman, and J. L. Wilson, 1984, Closed system marine burial diagenesis— isotope data from the Austin chalk and its components: Sedimentology, v. 31, p. 863–877.

De Cserna, Z., 1989, An outline of the geology of Mexico, *in* A. W. Bally and A. R. Palmer, eds., The Geology of North America— an overview: Geological Society of America, The geology of North America, v. A, p. 233–264.

Escalera-Alcocer, A., V. M. Valdivieso-Ramos, and R. Rhame-Escobedo, 1997, Development of the Mata Pionche field, Zongolica fold and thrust belt, Mexico (Abs.): AAPG/Asociación Mexicana de Geólogos Petroleros International Research Symposium, Oil and gas exploration and production in fold and thrust belts, Veracruz, Mexico, Poster Session III, 4 p.

Feng, J., R. T. Buffler, and M. A. Kominz, 1995, Laramide orogenic influence on Late Mesozoic–Cenozoic subsidence history, Western Deep Gulf of Mexico Basin: Geology, v. 22, p. 359–362.

Ferket, H., S. Ortuño-Arzate, F. Roure, and R. Swennen, 2003, Lithologic control on matrix porosity in shallow-marine Cretaceous reservoir limestones: A study of the Peñuela Reservoir outcrop analog (Cordoba Platform, Southeastern Mexico), *in* C. Bartolini, R. T. Buffler, and J. Blickwede, eds., The Circum-Gulf of Mexico and the Caribbean: Hydrocarbon habitats, basin formation, and plate tectonics: AAPG Memoir 79, p. 283–304.

Frank, T. D., and M. A. Arthur, 1999, Tectonic forcings of Maastrichtian ocean-climate evolution: Paleoceanography, v. 14-2, p. 103–117.

Freeland, G., and R. Dietz, 1971, Plate tectonic evolution of the Caribbean–Gulf of Mexico region: Nature, v. 232, p. 20–23.

Frizon de Lamotte, D., E. Mercier, A. Dupré La Tour, P. Robion, and O. Averbuch, 1997, Cinématique du plissement et déformation interne des roches. L'exemple du pli de Lagrasse (Aude, France): Conseil de la Recherche, Académie des Sciences, Paris, v. 324, p. 591–598.

Gonzalez Alvarado, J., 1976, Resultados obtenidos en la exploracion de la plataforma de Cordoba y principales campos productores: Boletín de la Sociedad Geológico Mexicana, v. 378, p. 53–59.

Gonzalez, R., and I. N. Holguin, 1992, Geology of the source rocks of Mexico: Proceedings, 13th World Petroleum Congress, Buenos Aires, v. 2, p. 95–104.

Guzman-Vega, M., and M. R. Mello, 1994, Genetic assessment of hydrocarbons in Southeastern Mexico. AAPG/AMGP Research Conf., Mexico, October 2–6, Abs.

Holguin-Quiñones, N., and J. R. Roman-Ramos, 1997, HC generative subsystems of the productive Mexican basins (Abs.): AAPG/ Asociación Mexicana de Geólogos Petroleros Research Conference, Mexico City, October 2–6, p. 23–32.

Jacobo, A. J., 1995, Studio geologico y petrologico del massicio vulcanico i los Tuxtlas: Ph.D. Thesis, Universitá degli study i Pisa, Italy, 455 p.

López, R. E., 1979, Geología de México, Edición Escolar, Mexico D.F., 446 p.

Menes, S., 1980, Estudio Estratigráfico y Sedimentológico del Cretácico Medio y Superior. Prospecto Tezonapa: PEMEX, Reporte Interno Inédito.

Molnar, P., and L. R. Sykes, 1969, Tectonics of the Caribbean and Middle America regions from focal mechanisms and seismicity: Geological Society of America Bulletin, v. 80, p. 1639–1684.

Moore, G. W., and L. del Castillo, 1974, Tectonic evolution of the southern Gulf of Mexico: Geological Society of America Bulletin, v. 85, p. 607–618.

Mossman, R. W., and F. Viniegra, 1976, Complex fault structures in Veracruz Province of Mexico: AAPG Bulletin, v. 60, p. 379–388.

Ortega-Gutierrez, F., L. M. Mitre-Salazar, J. Roldán-Quintana, G. Sánchez-Rubio, and M. De la Fuente, 1990, North American Continent–Ocean Transect Program, Transect H-3— Acapulco Trench to the Gulf of Mexico across southern Mexico: Geological Society of America, Decade of North American Geology Program, map and sections, scale 1:500,000, 9 p.

Ortuño, S., 1989, La sédimentation mésozoïque dans le Bassin de Zongolica (Mexique central): Colloque Association de Sédimentologistes Français, Paris, p. 217.

Ortuño, S., 1991, Contribution de la sédimentologie et de la télédétection à la reconstitution de l'évolution du Bassin de Zongolica (Mexique centro-oriental). Place dans la dynamique du couple Golfe du Mexique/ système cordillérain: Ph. D Thesis, Université de Pau et des Pays de l'Adour, France, 289 p.

PEMEX-IMP, 1995, Estudio tectónico del Cinturon Plegado y Cabalgado de Zongolica y de la Cuenca Terciaria de Veracruz: PEMEX-IMP, Reporte Interno Inédito.

Pindell, J., and J. F. Dewey, 1982, Permo-Triassic reconstruction of western Pangea and the evolution of the Gulf of Mexico-Caribbean region: Tectonics, v. 1, p. 179–211.

Pottorf, R., G. G. Gray, M. G. Kozar, W. M. Fitchen, M. Richardson, R. J. Chuchla, and D. A. Yurewicz, 1996, Hydrocarbon generation and migration in the Tampico segment of the Sierra Madre Oriental fold-thrust belt: Evidence from an exhumed oil field in the Sierra de El Abra: Memoria del V Congreso Latinoamericano de Geoquimica Organica, p. 100–101.

Reed, J. M., 1994, Probable Cretaceous-to-Recent rifting in the Gulf of Mexico Basin, Part I: Journal of Petroleum Geology, v. 17, no. 4, p. 629–666.

Rodriguez, D., J. Toriz, J. Banda, and J. Meneses-Rocha, 1997, Hydrocarbon habitat in the Zongolica sector of the Sierra Madre Oriental (Abs.): AAPG/AMPG International Research Symposium, Oil and gas exploration and production in fold and thrust belts, Veracruz, Mexico, Oral Session III, p. 2–7.

Roure, F., R. Swennen, and D. G. Howell, 2000, Subtrust reservoir appraisal: World Petroleum Conference, proceedings, Calgary, Alberta, Canada.

Salvador, A., 1987, Late Triassic-Jurassic paleogeography and origin of Gulf of Mexico Basin: AAPG Bulletin, v. 71, p. 419–451.

Salvador, A., 1991, Origin and development of the Gulf of Mexico basin, *in* A. Salvador, ed., The Gulf of Mexico Basin: Geological Society of America, The geology of North America, v. J, p. 389–444.

Sassi, W., and J. L. Faure, 1997, Role of faults and layer interfaces on the spatial variation of stress regimes in basins: Inferences from numerical modelling: Tectonophysics, v. 266, p. 101–119.

Sedlock, R. L., F. Ortega-Gutierrez, and R. C. Speed, 1993, Tectonostratigraphic terranes and tectonic evolution of Mexico: Geological Society of America Special Paper 278, 153 p.

Suter, M., 1991, State of stress and active deformation in Mexico and western Central America: Geological Society of America, The geology of North America, Decade Map v. 1, p. 401–421.

Swennen, R., and M. Dusar, 1997, Diagenesis of Late Cretaceous to Paleocene carbonates in the Ruhr Valley Graben (Molenbeersel borehole, NE-Belgium): Annales de la Société géologique du Nord, v. 5, 2e série), p. 215–226.

Toriz, G. J., 1985, Prospecto Tehuipango: PEMEX, Reporte Interno Inédito.

Toriz, G. J., 1987, Prospecto Chapulco-Atzompa: PEMEX, Reporte Interno Inédito.

Wadge, G., and K. Burke, 1983, Neogene Caribbean plate rotation and associated Central American tectonic evolution: Tectonics, v. 2, p. 633–643.

Walper, J. L., and C. L. Rowett, 1972, Plate tectonics and the origin of the Caribbean Sea and Gulf of Mexico: Gulf Coast Association of Geological Societies Transactions, v. 22, p. 105–116.

Winkler, C. D., and R. T. Buffler, 1988, Paleogeographic evolution of early deep-water Gulf of Mexico and margins, Jurassic to Middle Cretaceous (Coman-Chean): AAPG Bulletin, v. 72, p. 318–346.

Yurewicz, D. A., R. J. Chuchla, R. J. Pottorf, G. G. Gray, M. Richardson, M. G. Kozar, and W. M. Fitchen, 1997, Hydrocarbon generation and migration in the Tampico segment of the Sierra Madre Oriental fold-thrust belt: Evidence from an exhumed oil field in the Sierra de El Abra (Abs.): AAPG/AMPG International Research Symposium, Oil and gas exploration and production in fold and thrust belts, Veracruz, Mexico, Oral Session I, p. 11–15.